# Techno-economic comparison of three technologies for pre-combustion CO$_2$ capture from a lignite-fired IGCC

Simon Roussanaly[a,*], Monika Vitvarova[b], Rahul Anantharaman[a], David Berstad[a], Brede Hagen[a], Jana Jakobsen[a], Vaclav Novotny[b] and Geir Skaugen[a]

[a]*SINTEF Energy Research, Sem Sælandsvei 11, NO-7465 Trondheim, Norway*

[b] *Czech Technical University in Prague, Faculty of Mechanical Engineering, Technicka 4, 166 07  Prague 6, Czech Republic*

* Corresponding author. Tel.: +47 47441763; fax: +47 735 97 250; E-mail address: simon.roussanaly@sintef.no

## Abstract

This paper compares the techno-economic performances of three technologies for CO$_2$ capture from a lignite-based IGCC power plant located in the Czech Republic: 1) Physical absorption with a Rectisol-based process 2) Polymeric CO$_2$-selective membrane-based capture 3) Low-temperature capture.

The evaluations show that the IGCC plant with CO$_2$ capture leads to costs of electricity between 91 and 120 €.MWh$^{-1}$, depending on the capture technology employed, compared to 65 €.MWh$^{-1}$ for the power plant without capture. This results in CO$_2$ avoidance costs ranging from 42 to 84 €.t$_{CO2,avoided}^{-1}$ , mainly linked to the losses in net power output. From both energy and cost points of view, the low-temperature and Rectisol based CO$_2$ capture processes are the most efficient capture technologies.

Furthermore, partial CO$_2$ capture appears as a good mean to ensure early implementation due to the limited increase in CO$_2$ avoidance cost when considering partial capture. To go beyond the two specific CO$_2$-selective membranes considered, a cost/membrane property map for CO$_2$-selective membranes was developed. This map emphasise the need to develop high performance membrane to compete with solvent technology. Finally, the cost of the whole CCS chain was estimated at 54 €.t$_{CO2,avoided}^{-1}$ once pipeline transport and storage are taken into consideration.

*Keywords:* Carbon Capture and Storage (CCS); Techno-economic comparison; Pre-combustion capture; Physical solvent; Polymeric membrane; Low-temperature capture.

Abbreviations: AACE, Association for the advancement of cost engineering ; ASU, Air separation unit; CAC, CO$_2$ avoidance cost; CCR, carbon capture ratio; CCS, carbon capture and storage; CEPCI, chemical engineering plant cost index; DC, direct cost; EBTF, European benchmarking task force; EPC, engineering, procurement, construction; EPCCI, European power capital costs index; HRSG, Heat recovery steam Generator; IGCC, integrated gasification combined cycle; KPI, key performance indicator; LCOE, levelised costs of electricity; MDEA, mono-diethanolamine; NCCC, National carbon capture center; NETL, national energy technology laboratory; NOAK, n[th] of a kind; OPEX, operating expenditures; PSA, pressure swing adsorption; TPC, total plant costs; WGS, water gas shift.

## 1    Introduction

Due to its local availability and its low cost, lignite is especially used in the power generation sector in Germany, United States, Russia, Central and Eastern Europe. While lignite still represents around 10% of the total world coal production, the global demand for lignite has been decreasing for the last decades [1]. In 2015, however a pause in this trend has been observed due to low energy prices in Europe. If this pause continues, it could compromise the objective of European countries to limit the global temperature increase well below 1.5 ºC [2] if CCS is not integrated to lignite-fired power plants.

While post-combustion electricity generation is more cost-efficient than the pre-combustion route, lignite-fired integrated gasification combined cycle (IGCC) opens the way to poly-generation: electricity, syngas and hydrogen which can be used for various types of application (power, chemical, fuel). Moreover, the high $CO_2$ content and pressure of the syngas make pre-combustion a potentially interesting route for cost-efficient $CO_2$ capture [3].

Although solvent-based $CO_2$ capture is the most mature and demonstrated technology for $CO_2$ capture, other emerging technologies such as membrane, cryogenic separation, precipitating solvents, adsorption, and oxy-combustion have the potential to significantly reduce costs in the long run [4, 5]. $CO_2$ capture from a coal-fired IGCC with solvent-based technology [6, 7] or the comparative assessments of a specific emerging capture technologies with solvents have been extensively studied [3, 8]. Urech et al. [9] compared $CO_2$ capture from a black coal IGCC with three solvent technologies: mono-diethanolamine (MDEA), hot potassium carbonate and Selexol. They concluded that the power plant with hot potassium carbonate $CO_2$ capture process yielded the highest efficiency (37.33%) compared to the Selexol- (36.42%) and MDEA- (36.39%) based capture processes. The European Benchmarking Task Force (EBTF) has assessed the technical and economic performances of a power plant with and without Selexol-based $CO_2$ capture [10]. Their cost estimates identified levelised costs of electricity (LCOE) of 64.6 and 86 €.MWh$^{-1}$ respectively for the power plant without and with $CO_2$ capture, resulting in a $CO_2$ avoided cost of 33 €.t$_{CO2, avoided}$$^{-1}$. Zhai and Rubin [11] investigated the potential of an ionic liquid solvent, based on 1-hexyl-3-methylimidazolium bis(trifluoromethylsulfonyl)imide, for $CO_2$ capture from an IGCC. They concluded that the ionic liquid resulted in a $CO_2$ capture cost of 62 $.t$_{CO2}$$^{-1}$, thus in the similar range than Selexol for the IGCC case considered. Gazzani et al. [12] have estimated the $CO_2$ capture cost from an IGCC with a Palladium membrane at 55 €.MWh$^{-1}$ for a process with a state-of-the-art lock hopper, while this cost could be reduced to an optimistic 35 €.MWh$^{-1}$ with an advanced lock hopper. Lin et al. [10] assessed the $CO_2$ capture cost from a TRIG IGCC with the $CO_2$-selective membrane Polaris to 63 $.t$_{CO2,avoided}$$^{-1}$. Meanwhile, Grainger and Hägg [13] concluded that $CO_2$ capture from a IGCC power plant based on a fixed site carrier $CO_2$-selective membrane would result in a $CO_2$ avoidance cost (CAC) of 40 €.t$CO2,avoided$$^{-1}$. Berstad el al. [3] evaluated that low-temperature based $CO_2$ capture from an IGCC would result in a CAC of 23 €.t$_{CO2,avoided}$$^{-1}$, leading to a cost reduction of 35% compared with Selexol-based capture. Finally, Riboldi and Bolland [14] performed a comprehensive comparative performance analysis of $CO_2$ capture with a pressure swing adsorption process (PSA) from an IGCC with Selexol-based capture. They found that neither modifications in the process nor in the material were able to fully close the gap with Selexol-based capture.

However, a rather limited number of papers have investigated $CO_2$ capture from lignite-fired IGCC plants with conventional solvent technologies or emerging technologies [15]. Moreover, no systematic cost-comparisons of various $CO_2$ capture technologies from a lignite-fired IGCC have been carried out.

This study therefore presents a techno-economic comparison, for a lignite-based IGCC plant, of three pre-combustion $CO_2$ capture technologies: 1) physical absorption in a Rectisol-based process 2) Polymeric membrane-based capture considering $CO_2$-selective membranes 3) Low-temperature capture.


## 2    Methodology
### 2.1    Study concept and system boundaries
The aim of this study is to assess and compare three technologies for $CO_2$ capture from a lignite-fired IGCC power plant based on both energy and cost performances. The three $CO_2$ capture technologies (physical absorption in a Rectisol-based process, polymeric membrane-based capture, and low-temperature capture) are considered to capture around 85% of the $CO_2$ from the syngas that would otherwise have been emitted by the power plant. In addition, the performances of the power plant without $CO_2$ capture are also evaluated to provide a reference point, as well as calculate the CAC [16] of the different concepts.

The system boundaries include the whole power plant with $CO_2$ capture and conditioning as presented in Figure 1. The main inputs to the plant are the lignite and other utilities (such as water, solvent, etc.). In the base case, the carbon capture ratio (CCR), corresponding to the percentage of carbon extracted from

the syngas, including both $CO_2$ and CO, is set to 85% [17-19]. The captured $CO_2$, with a purity of at least 95% [20], is then conditioned in order to meet the conditions required for pipeline transport and storage, while the remainder of the exhaust flue gas is vented. The $CO_2$ conditioning process consists of compression stages and pumping in order to reach a pressure of 110 bar [20, 21].
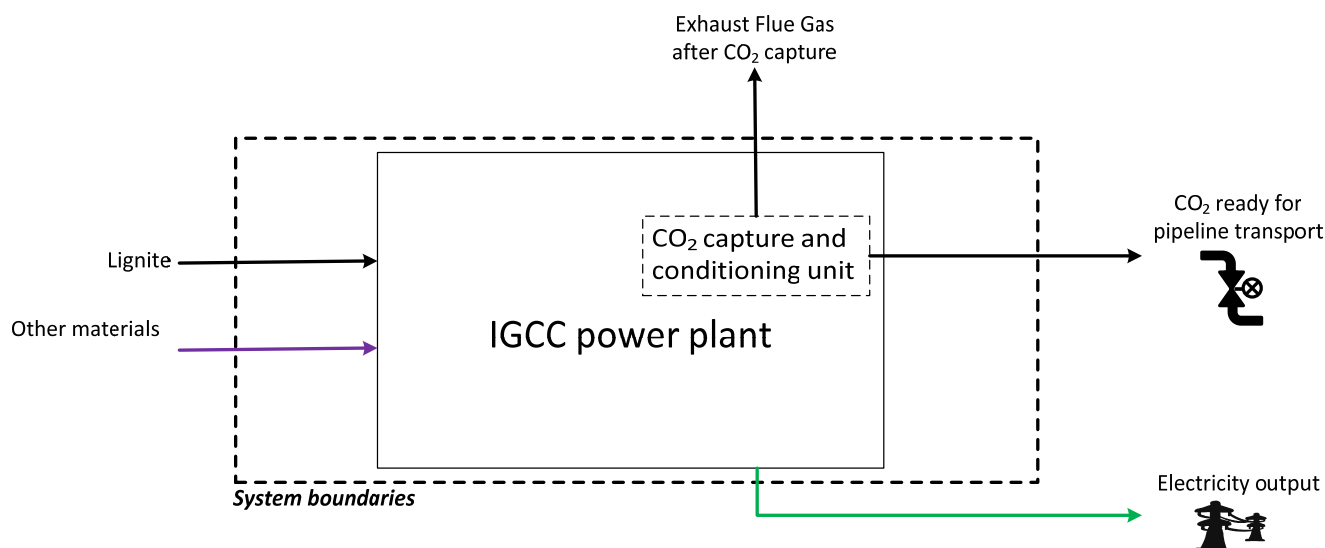


Figure 1: System boundaries of the IGCC power plant with $CO_2$ capture and conditioning

## 2.2 Technical modelling
### 2.2.1 Technical modelling of the IGCC plant

The reference IGCC plant considered in this study is based on a dry coal-fed oxygen-entrained flow gasifier (Shell configuration) similar to the Vřesová IGCC plant in the Czech Republic. The IGCC plant is fed with 39 $kg_{wet}.s^{-1}$ of lignite with the characteristic as shown in Table 1, leading to a net power output of 278 MW for the plant without $CO_2$ capture. A generic process flow diagram of the IGCC plant without $CO_2$ capture is presented in Figure 2.

The dried pulverised coal is pneumatically conveyed by inert nitrogen gas from the Air Separation Unit (ASU) into the gasifier, which is also fed by compressed oxygen supplied by the ASU. Radiant coolers are used within the gasifier wall to cool the syngas and produce high pressure steam. The syngas is further quenched (gas quench by recycled syngas) to 900 °C and cooled in convective coolers producing high and medium pressure saturated steam, before passing through filters for fly ash removal. A desulphurisation system to remove $H_2S$ (acid gas removal, AGR) follows. The clean fuel gas is burned in a gas turbine (parameters based on SGT-2000E, 187 MWe of nominal output). The turbine exhaust gas is used in a Heat Recovery Steam Generator (HRSG) for a dual-pressure steam cycle. The IGCC plant is modelled in Aspen Plus® using the Peng-Robinson equation of state for properties formulation, except for the gasifier, where using the Redlich-Kwong-Soave equation of state is recommended [22].

When $CO_2$ capture from the plant is included, the reference IGCC is modified to include two major adjustments. First, water gas shift (WGS) units are included to convert the CO present in the syngas into $CO_2$ so that the heating value is transferred into creation of hydrogen fuel and $CO_2$ which can be captured. The second major modification consists of adding nitrogen from the ASU to the hydrogen-rich fuel as a diluent in order to limit the gas turbine temperature and ensure safe and efficient turbine operation. The characteristics of lignite as received and at the outlet of the fluidised bed dryer are shown in Table 1. The syngas characteristics after the WGS are presented in Table 2, while the hydrogen-rich syngas and $CO_2$ specifications after the $CO_2$ capture units are presented in Table 3 and Table 4. A generic process flow diagram of the IGGC plant with $CO_2$ capture is provided in Figure 3.

3
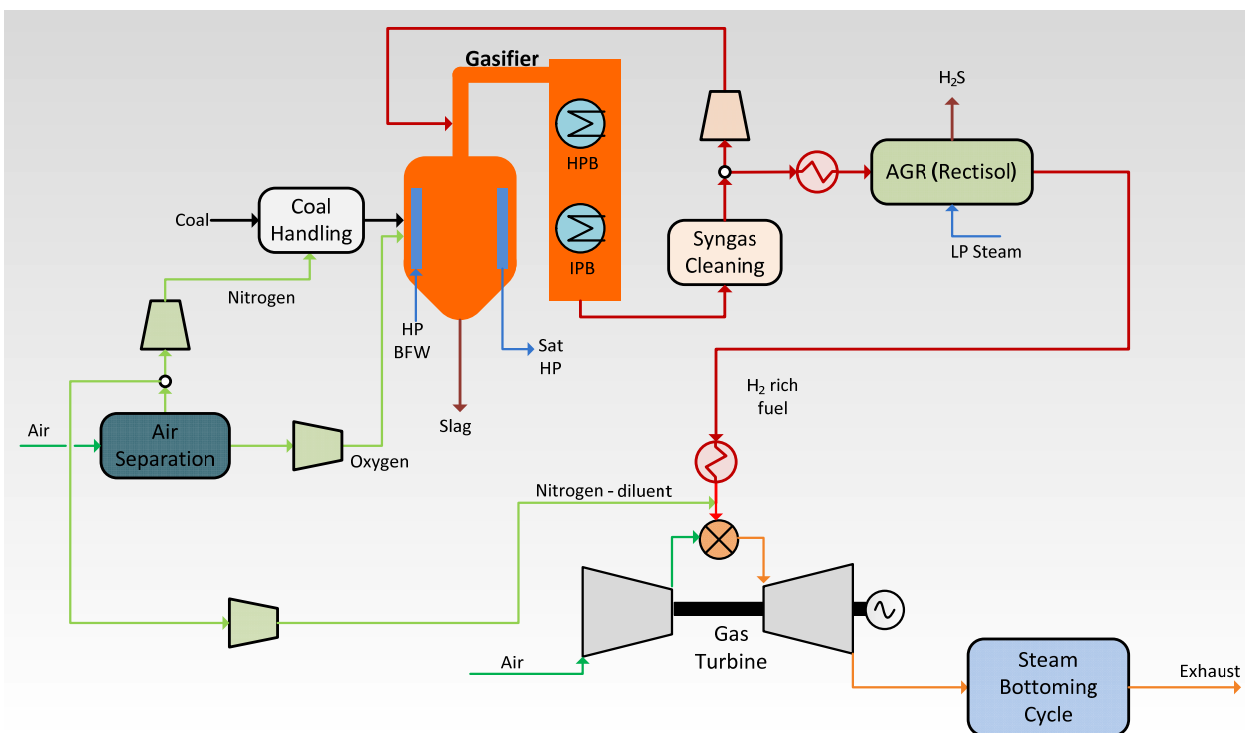
Figure 2: Generic Process Flow Diagram of the IGCC plant without $CO_2$ capture
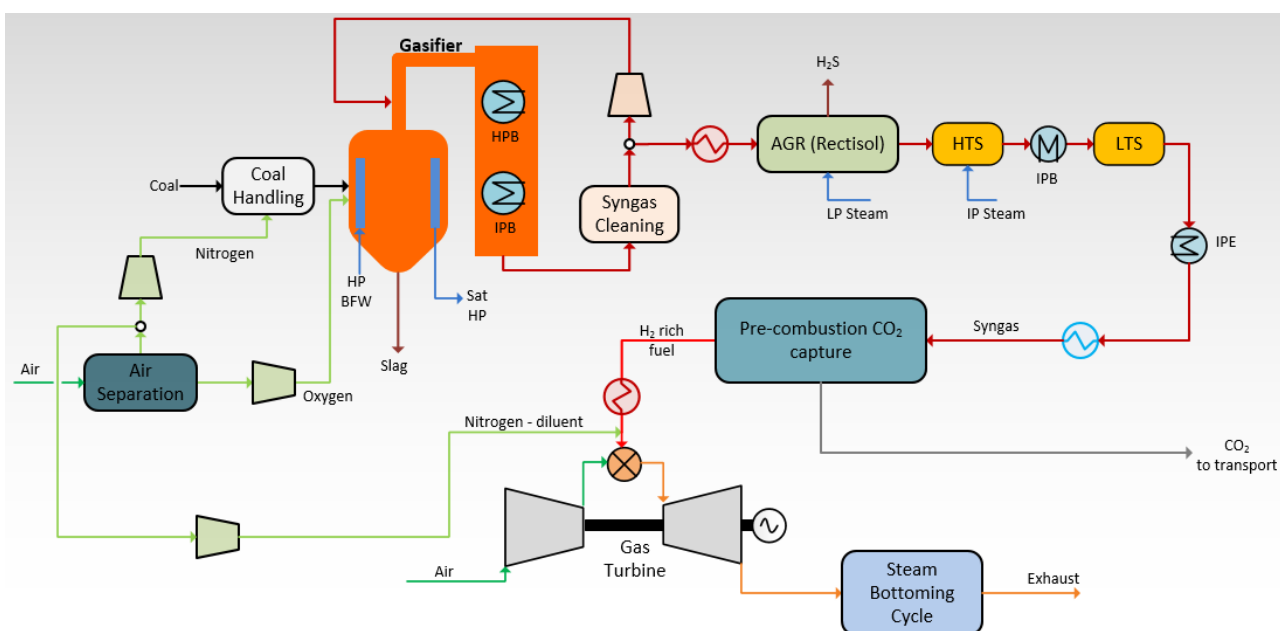


Figure 3: Generic Process Flow Diagram of the IGCC plant with $CO_2$ capture

Table 1: Lignite characteristics

|  | As received | dried |
|---|---|---|
| LHV /MJ.kg$^{-1}$ | 16.50 | 21.99 |
| HHV /MJ.kg$^{-1}$ | 18.07 | 23.31 |
| Moisture /wt% | 31.00 | 11.00 |
| Ash /wt% | 8.97 | 11.57 |
| Carbon /wt% | 42.26 | 54.51 |
| Hydrogen /wt% | 3.66 | 4.72 |
| Nitrogen /wt% | 0.60 | 0.77 |
| Oxygen /wt% | 12.54 | 16.18 |
| Sulphur /wt% | 0.97 | 1.25 |

4

Table 2: Syngas characteristics after the WGS unit

| Component | Concentration /vol% | | Parameters | Value |
|---|---|---|---|---|
| CO | 1.08 | | Mass flow /kg.s$^{-1}$ | 68 |
| CO$_2$ | 38.64 | | Pressure /bar | 28.4 |
| H$_2$ | 53.41 | | Temperature /°C | 30 |
| N$_2$ | 5.89 | | | |
| Ar | 0.80 | | | |
| Other | 0.18 | | | |

* H$_2$O, HCL, COS, CH$_4$, etc.

Table 3: Specifications of the hydrogen rich fuel

| Component | Concentration /vol% |
|---|---|
| H$_2$ | > 80 |
| CO | < 2.5 |
| CO$_2$ | < 8 |
| H$_2$S /ppm | < 30 |

Table 4: Specification of the CO$_2$ product

| Component | Concentration /vol% | | Parameters | Value |
|---|---|---|---|---|
| CO$_2$ | > 95 | | Pressure /bar | 110 |
| H$_2$ | < 3* | | Temperature /°C | 40 |
| N$_2$ | < 3* | | | |
| Ar | < 3* | | | |
| O$_2$ | < 3* | | | |
| CO /ppm | < 2000 | | | |
| H$_2$S /ppm | 100 | | | |
| H$_2$O /ppm | 300 | | | |

* All non-condensable gases (H$_2$+N$_2$+Ar+O$_2$ <3 vol%)

## 2.2.2 Technical modelling of the CO$_2$ capture and conditioning processes

The three CO$_2$ capture technologies evaluated in this study are described below.

### 2.2.2.1 Rectisol-based CO$_2$ capture

Solvent-based CO$_2$ capture, as well as H$_2$S removal, in pre-combustion processes can be achieved by various solvents (Rectisol, Selexol, Purisol, etc.). In IGCC plants, the most common technologies used are the Selexol process and Rectisol process (methanol solvent). The Rectisol technology presents several advantages compared to competing solvents: higher loading (absorption capacity), higher thermal and chemical stability, non-foaming properties, absence of degradation, minimal corrosion, low H$_2$ loss from the system and local technology experience at the Vřesová IGCC plant for H$_2$S removal. However, it is also worth noting that Rectisol also presents several drawbacks: higher energy requirement, lower selectivity between H$_2$S and CO$_2$, sub-zero operating temperatures, and higher solvent loss [23-27].

The Rectisol separation process is here chosen for both H$_2$S removal and CO$_2$ capture, especially due to the strong experience at the Vřesová plant. Even though a combined H$_2$S and CO$_2$ separation after the water-gas-shifts could be considered [9, 23, 27] , the study assumes a H$_2$S separation upstream of the WGS units as it has been identified as a more energy-efficient option, due to methanol solvent properties and the rather high sulphur content of the coal. The capture process is modelled in AspenPlus based on equilibrium columns. The desorption of H$_2$S is realised as combined flashing and distillation, while the desorption of CO$_2$ (see Figure 4) is based on flashes at multiple pressure levels. The CO$_2$ streams are then compressed by four or five compression stages (depending on CCR and thus number of flash drums needed) with successive additions of CO$_2$ from higher pressure flash drums and intercooling. After each compression stage, major condensed impurities such as methanol are separated and recycled.

Water has a very high affinity for methanol and, if present in the syngas, could accumulate in the methanol loop and lead to freezing problems due to the low temperatures employed (around -20 °C). Therefore, pre-absorption is necessary to remove nearly all of the water through scrubbing with a small amount of methanol, which is then regenerated by distillation with low energy requirement.

5

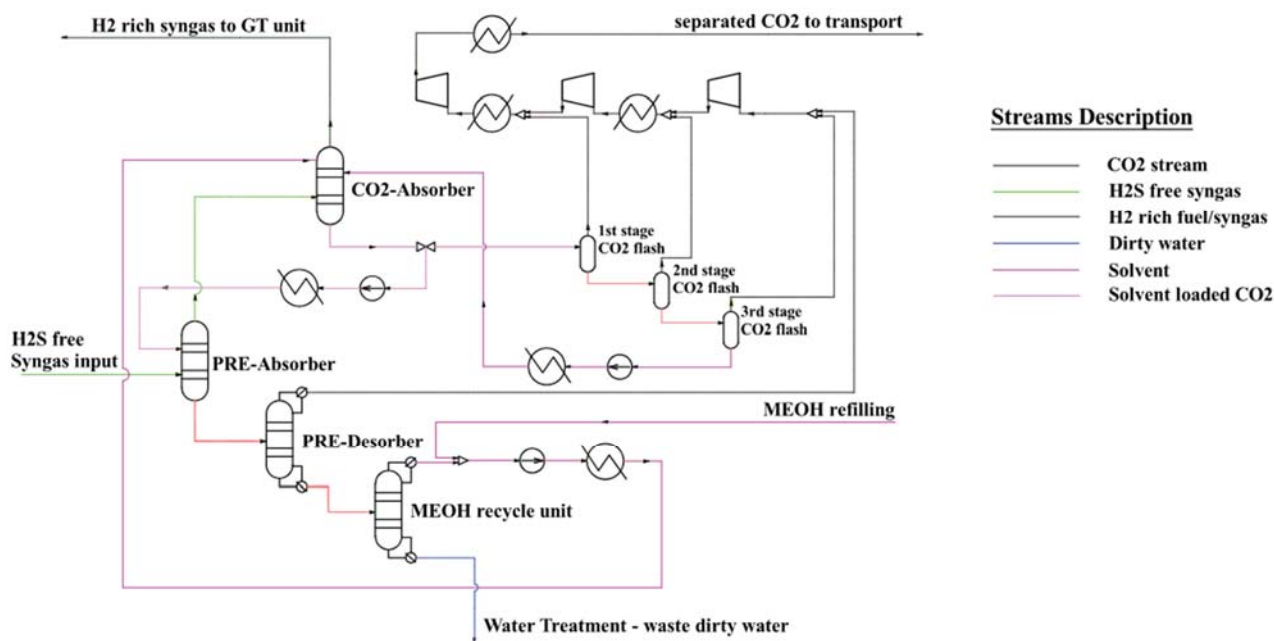Figure 4 shows the process flow diagram of the Rectisol process for $CO_2$ capture.



Figure 4: Process Flow Diagram of the Rectisol process for $CO_2$ capture

## 2.2.2.2 Polymeric membrane-based $CO_2$ capture

Although some inorganic $H_2$-selective membranes seem to have a stronger cost reduction potential, polymeric $CO_2$-selective membranes are at a higher stage of development [4].

In practise, several process designs for $CO_2$ capture are possible depending on membrane types, process layout and level of complexity. Here, "simple" single-stage and two-stage separation processes are considered in this work. The process layout of a two-stage processes based on $CO_2$-selective membranes is shown in Figure **5**. Based on literature, two $CO_2$-selective membranes available or under development, with the characteristics presented in Table 5, are evaluated. Membrane A corresponds to a $CO_2$-selective membrane developed by Membrane Technology Research and which has been tested at the National Carbon Capture Center (NCCC) in Wilson, Alabama. [28] . Membrane B corresponds to an amine modified PVAm membrane which has higher permeance and selectivity than membrane A, but is still in the early development phase [29].

In each case, the membrane process is optimised so as to minimise the cost of electricity for a given fixed recovery ratio of carbon ($CO_2$ and CO), based on a numerical version of the Attainable Region Approach [30-32]. The process variables taken into account during the optimisation process are the permeate pressures of each membrane stage and the feed pressure of the second membrane stage. The feed pressure of the first membrane stage is known, as it is assumed that no compression takes place before the first stage due to the inherent high syngas pressure. The membrane area(s) are computed to ensure a fixed carbon recovery ratio (stage cut) in each stage.

The membrane module is modelled as a two-components separator in cross-flow configuration with negligible mixing on the permeate side [33]. The use of a two-components model is commonly considered in literature[34-36] as very often experimental studies only report the $CO_2$/$H_2$ selectivity [29, 37, 38]. Here, all components other than $CO_2$ are lumped together with hydrogen.

Table 5: $H_2$ and $CO_2$ selective membranes considered and their characteristics

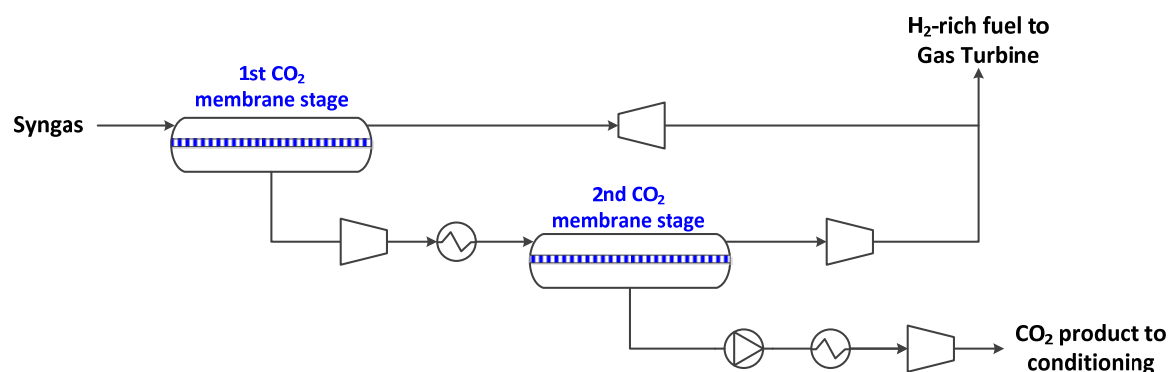| Membrane | Selectivity | $CO_2$ permeance |
| --- | --- | --- |
| | /- | /$m^3_{(STP)}.m^{-2}.h^{-1}.bar^{-1}$ |
| Membrane A [39] | 10 | 2.7 |
| Membrane B [29] | 63 | 7 |



Figure 5: Layout of a two stages membrane-based $CO_2$ capture process based on $CO_2$ selective membranes

### 2.2.2.3 Low-temperature $CO_2$ capture

In addition to the aforementioned physical solvents and membrane separation, $CO_2$ can also be captured by compression, condensation and vapour-liquid separation in successive order. Condensation of $CO_2$ from the syngas stream is possible since the $CO_2$ concentration and partial pressure are sufficiently high [40] and the efficiency of this type of separation process increases sharply with $CO_2$ concentration and syngas pressure. In contrast to the Rectisol process, for example, this technology has not yet been commercialised, but shows promising competitiveness for suitable applications [3, 41-43].

The low-temperature capture process separates condensed $CO_2$ from the hydrogen-rich gaseous phase of the syngas in vapour-liquid separators, and the obtainable CCR is constrained by the vapour-liquid equilibrium conditions for the syngas composition at the targeted separation pressure and temperature. The actual CCR depends on the degree of equilibrium obtained in the heat exchangers and separation vessels.

Figure **6** shows the process scheme for the low-temperature separation unit. In order to avoid ice formation at sub-zero temperatures, which could obstruct channels in heat exchangers, the syngas is dehydrated prior to entering the condensation unit. After dehydration, the syngas is compressed to the required separation pressure, which is dependent on the targeted CCR. From the aftercooler of the compressor train, the syngas stream enters a heat exchanger network made up of both process-to-process heat recuperators and auxiliary refrigeration exchangers. Refrigerants in the auxiliary process are assumed to be propane and ethane, although other refrigerants such as ammonia and $CO_2$ may be used.

The syngas temperature at the outlet of the last heat exchangers is set to -55 °C, but could be increased if a higher margin to the $CO_2$ freeze-out temperature is desired. At this point a considerable fraction of the $CO_2$ content has condensed and is separated in the main separator. The liquid stream is subsequently heated and throttled back to -55 °C at a considerably lower pressure level, around 8 bar, and is hence further purified before it is pressurised by liquid pumping and heated against the feed stream. Flash gas from the second separator contains a significant fraction of hydrogen, and can be recycled back into the feed. The largely decarbonised hydrogen-rich gas product from the first separator is heated against the feed stream. Due to the large difference between separation pressure and the hydrogen fuel target pressure, this stream can also be expanded in order to maximise the internal heat recuperation as well as to recover a considerable amount of power to lower the net power requirement.
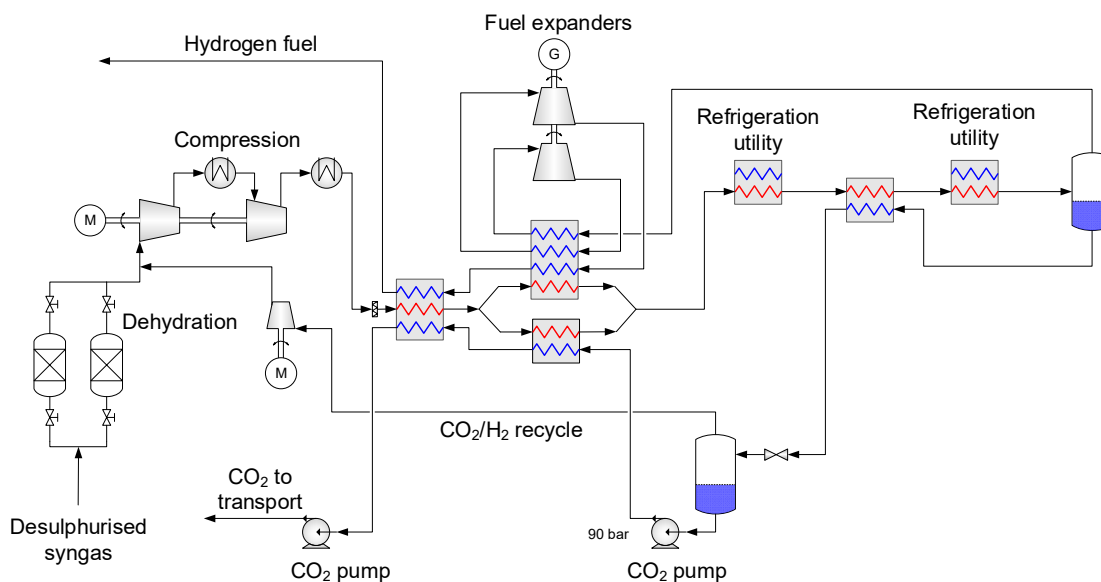
Figure 6: Process Flow Diagram of the low-temperature unit for separation

## 2.3 Cost evaluation of the power plant with and without $CO_2$ capture

While the costs of the power plant without $CO_2$ capture are modelled based on the EBTF report [10], the costs of the $CO_2$ capture and conditioning processes are evaluated based on a Bottom-Up Approach presented below.

Most studies evaluate and compare $CO_2$ capture technologies on an $N^{th}$ Of A Kind (NOAK) basis, assuming the various technologies to be mature and proven [10, 34, 44, 45]. However these technologies are currently at different levels of both maturity and demonstration [4]. This study therefore considers the evaluation and comparison of the $CO_2$ capture technologies both at their current level of maturity, following the AACE and NETL guidelines [46, 47] as well as on a NOAK basis.

Investment and operating costs are given in 2015 Euro prices and for a plant located in the Czech Republic. As the costs available in the EBTF report are for 2008 price levels, the investments of the power plant have been updated according to the European Power Capital Costs Index (EPCCI), excluding nuclear power[1] [48], while relevant utility costs are corrected according to an average annual inflation rate of 1.7% [49].

### 2.3.1 Investment costs

A factor estimation method is used to estimate the investment costs of the process equipment, where the direct costs estimated for each item of equipment are multiplied by indirect[2] cost factors to obtain the total plant costs (TPC).

While the direct costs of the power plant are scaled from the EBTF, the direct costs (DC) without process contingencies of the $CO_2$ capture and conditioning processes are estimated for a Netherlands-based plant based on the process designs of the three different capture processes and Aspen Process Economic Analyzer®. However, due to its specificity, the membrane module and framework direct costs are estimated assuming a cost of $700 €_{2014}.m^{-1}$ as suggested by Lin et al. [8]. The direct costs of both the power plant and the $CO_2$ capture and conditioning plant are updated to reflect the costs of a plant located in the Czech Republic [50]. The total plant cost is obtained by adding process contingencies, indirect costs, owner's costs and project contingencies to the direct costs without contingencies. The process contingencies are based on the AACE guidelines for process contingency [46] and shown in Table 6. While the indirect costs are assumed to be equal to $14\%_{DC}$ to be consistent with the EBTF, the owner's costs together with project contingencies are set to 19% of the Engineering, Procurement and Construction

---

[1] The EPCCI tracks and forecasts the costs associated with the construction of a portfolio of power generation plants in Europe, and as such, is an indicator of the market price of the power plants.
[2] Which includes the costs associated with engineering, commissioning, administration, and contingencies.

8

costs (EPC costs are equal to the direct cost including process contingencies and indirect costs), in the case of commercial technologies, following AACE 16R-90 guidelines for AACE Class 4 budget estimates [46, 51][3]. However, as most of the capture concepts considered in this study are not fully mature, the owner's costs and contingencies are corrected based on the level of maturity of each concept, as shown in Table 6 [47][4].

Table 6: Process contingencies, owner's costs and project contingencies used for the evaluation of the power plant with and without $CO_2$ capture

| Technology | Process contingency /%$_{DC\ without\ contingencies}$ [46] | TRL-level [4] | Owner's costs and project contingencies /%$_{EPC\ cost}$ [47] |
|---|---|---|---|
| IGCC plant (except gasifier) | Included in EBTF estimates | - | 19 |
| IGCC plant gasifier | Including in EBTF estimates + 10% | - | 24 |
| Rectisol $CO_2$ capture and $CO_2$ conditioning | 10 | 8 | 24 |
| Membrane $CO_2$ capture | 20 | 7 | 30 |
| Low-temperature $CO_2$ capture | 30 | 6 | 36 |

### 2.3.2 Maintenance and operating costs

The fixed operating costs include maintenance, insurance and labour costs. The cost of maintenance, insurance and local property taxes are assumed to be 4.5% of the EPC cost [10]. The operating labour cost is estimated based on the estimated overall number of employees and a "fully burdened" cost of labour of 40 k€.y$^{-1}$, while the administrative and support labour is assumed to be 30% of the operating labour combined with 12% of the maintenance cost, insurance and local property taxes [51, 52].

The variable operating costs include consumption of material utilities such as coal, process water, chemicals, sorbent, etc. The costs of the main utilities and consumables are evaluated based on the process energy and mass balance and the costs presented in Table 7. The costs of electricity and steam consumed in the power plant and the $CO_2$ capture are treated as internal utilities of the plant, and their costs are therefore taken into account via the plant net power output and efficiency.

Table 7: Costs of main utilities and consumables

| Utilities and consumables | Cost |
|---|---|
| Lignite /€.GJ$^{-1}$ [53] | 2 |
| Process water /€.m$^{-3}$ | 3.15 |
| Cooling water /€.m$^{-3}$ | 0.15 |
| Ash disposal /€.t$^{-1}$ | Not included |
| Sulphur credit /€.t$^{-1}$ | 0 |

### 2.3.3 Key Performance Indicators

Two Key Performance Indicators (KPI) are assessed here and used to compare the three capture technologies: the Levelised Cost Of Electricity (LCOE) [10] and the CAC [16].

The LCOE [€.MWh$^{-1}$] measures the unit cost of electricity generation of a plant with and without $CO_2$ capture, and approximates the average discounted electricity price over the project duration that would be required as income to match the net present value of the capital and operating costs of the project. It is equal to the annualised costs divided by the annualised net electricity production, as shown in equation (2). The LCOE is calculated on the assumption of a real discount rate of 8%[5] and an economic lifetime of 25 years [10]. In addition, investment costs assume that construction costs are shared over a three-year construction period following a 40/30/30 allocation [10]. Finally, capacity factors of 40% and 65% for

---

[3] AACE 16R-90 states that the project contingency for a "budget-type" estimate (AACE Class 4) should be 15% of the sum of the TDC (including process contingency) which, combined with the 7% of the TDC estimated for the owner's cost, leads to 19% of the EPC costs.
[4] Correction factors are estimated based on the learning curve approach suggested by NETL taking into account the differences in costs for the different maturity levels in the case of the 20$^{th}$ plant (which is assumed to have costs representative of the NOAK cases).
[5] This real discount rate of 8% corresponds to a nominal discount rate around 10% if an inflation rate of 2% is assumed.

the two first years of operation are applied in order to take potential technical issues into account, while a capacity factor of 85% can be achieved thereafter [10].

$$LCOE = \frac{\text{Annualised investment} + \text{Annual OPEX}}{\text{Annual net power output}} \qquad (2)$$

A second important KPI is the $CO_2$ avoidance (CAC) [$\text{€.tCO}_{2,\text{avoided}}^{-1}$], which is obtained by comparing the levelised cost and the $CO_2$ emission rate to the atmosphere of the plant with and without $CO_2$ capture, as shown in equation (3). The CAC approximates the average discounted $CO_2$ tax or quota over the duration of the project that would be required as income to match the net present value of additional capital and operating costs due to the CCS infrastructure. The CAC is used as the cost performance indicator to compare the different capture technologies. It is worth noting that the CAC is a better KPI than the LCOE to compare technologies with variations in capture ratio, as obtained here.

$$CO_2 \text{ avoidance cost} = \frac{(LCOE)_{CCS} - (LCOE)_{ref}}{(t_{CO2}/MWh)_{ref} - (t_{CO2}/MWh)_{CCS}} \qquad (3)$$

where
- $(LCOE)_{CCS}$ is the LCOE of produced by the plant with CCS [$\text{€.MWh}^{-1}$]
- $(LCOE)_{ref}$ is the LCOE of the reference plant without CCS [$\text{€.MWh}^{-1}$]
- $(t_{CO2}/MWh)_{CCS}$ is the $CO_2$ emission rate to the atmosphere of the plant with CCS [$.MWh^{-1}$]
- $(t_{CO2}/MWh)_{ref}$ is the $CO_2$ emission rate to the atmosphere of the reference plant without CCS [$.MWh^{-1}$]

It is worth noting that in sections 3.2, 4.1 and 4.2, the cost of $CO_2$ transport and storage are not included, and that the CAC corresponds to what is sometime called "cost of $CO_2$ captured" [16].

## 3    Results
The following sections present the results of the energy and techno-economic assessments.

### 3.1    Energy performances
While a detailed summary of the technical KPIs presented in Table 8 and details of the $CO_2$ capture processes are presented in Appendix , the gross and net power outputs of the power plant with and without CCS are presented in Figure 7. In the case of a power plant without capture, the results show that the power plant has a gross power output of 316.7, MW while a net power output of 275.6 MW is obtained once the auxiliary power consumption of the plant is taken into account.

Once the $CO_2$ capture is included, the assessment shows that the gross power output decreases by around 61-107 MW, depending on the $CO_2$ capture technology utilised. This drop in gross power output is explained by several effects of the power plant modification to incorporate the capture unit. First, the inclusion of WGS units to convert CO into $CO_2$ requires the consumption of large quantities of steam (36.5 $kg_{steam}.s^{-1}$) which results in a decrease of 22.4 MW in the steam turbine power output. Meanwhile the gas turbine power output decreases by 24-40 MW due to the lower calorific value of the $H_2$-rich fuel introduced by the limitation in the $H_2$ content of the standard gas turbine fuel gas, the reduced flow through the gas turbine, and the hydrogen losses in the $CO_2$ stream to transport and storage.

Once the auxiliary power consumption is taken into account, the net power output of the power plant with $CO_2$ capture and conditioning varies between 169 and 215 MW, depending on the capture technology employed. The assessment shows that Rectisol and low-temperature captures are the most energy-efficient $CO_2$ capture technologies among the ones considered. In the Rectisol case, the higher efficiency is due to its low $CO_2$ capture and conditioning power requirements. Indeed, the Rectisol-based capture is quite low (1.2 MW) as the regeneration is based on pressure release and does not require energy. However, this does result in higher conditioning power consumption (13.9 MW), as some of the $CO_2$ streams from the capture are obtained at lower pressures. In the case of the low-temperature capture, higher capture power consumption (13.9 MW) is required for the compression of the syngas to 103 bar in the process. However, in this case, the $CO_2$ conditioning is already integrated into the capture process. Finally, lower net power

outputs are obtained for membrane-based capture processes due to both higher capture and conditioning power requirements as well as lower gross power output. The higher capture and conditioning power requirements (45.6 and 24.5 MW for membranes A and B respectively) is due to both the feed compression and permeate vacuum pumping around the second membrane stage, as well as the significant power required to compress the captured $CO_2$ from 1 bar to the transport pressure. Furthermore, a lower gross power output than in the other capture cases is obtained as CO from the syngas also permeates through the membrane and is recovered together with the captured $CO_2$. It is worth noting that membrane B requires a much lower power consumption than membrane A, due to its significantly higher permeance and selectivity.
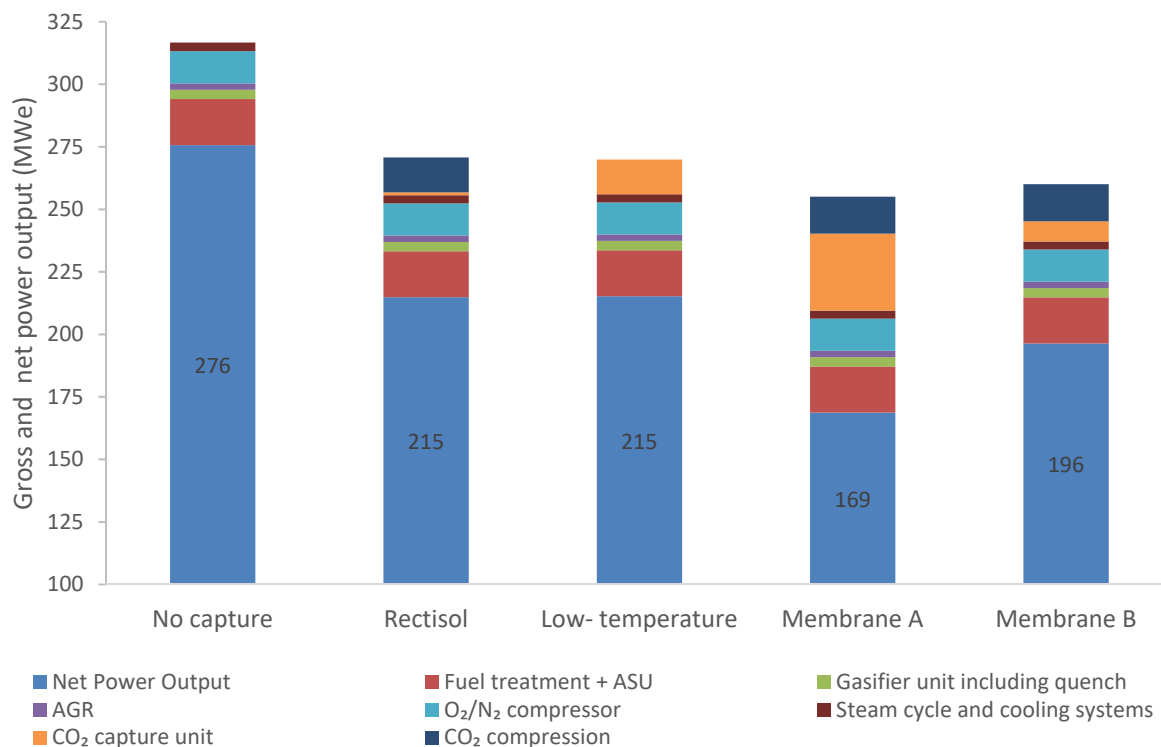


Figure 7: Net Power Output of the IGCC power plant with and without $CO_2$ capture and conditioning

Table 8: Key performance results from the process evaluations

| Parameters | No $CO_2$ capture | Rectisol capture | Low-temperature capture | Capture process based on membrane A | Capture process based on membrane B |
|---|---|---|---|---|---|
| Lignite Thermal Power input /$MW_{th}$ | 638.5 | 638.5 | 638.5 | 638.5 | 638.5 |
| Gas Turbine Net Power /$MW_e$ | 181.8 | 168.8 | 167.2 | 156.9 | 163.4 |
| Steam Turbine Gross Power /MWe | 134.8 | 101.9 | 102.7 | 95.0 | 96.6 |
| Gross power output /MWe | 316.7 | 270.7 | 269.9 | 255.1 | 260.0 |
| Fuel Treatment /MWe | 1.8 | 1.8 | 1.8 | 1.8 | 1.8 |
| ASU unit /MWe | 16.6 | 16.6 | 16.6 | 16.6 | 16.6 |
| $O_2/N_2$ compressors /MWe | 12.8 | 12.8 | 12.8 | 12.8 | 12.8 |
| Gasifier unit including quench (fans+compressors) /MWe | 3.7 | 3.7 | 3.7 | 3.7 | 3.7 |
| AGR unit /MWe | 2.6 | 2.6 | 2.6 | 2.6 | 2.6 |
| $CO_2$ capture unit /MWe | - | 1.2 | 13.9 | 30.7 | 8 |
| $CO_2$ conditioning unit /MWe | - | 13.9 | - | 14.8 | 14.8 |
| Steam Cycle Auxiliaries /MWe | 3.5 | 3.3 | 3.3 | 3.3 | 3.3 |
| Net Power Output /MWe | 275.7 | 214.8 | 215.2 | 168.7 | 196.3 |
| $CO_2$ capture ratio /% | - | 89.0 | 84.1 | 86.9 | 86.9 |

| | | | | | |
|---|---|---|---|---|---|
| CCR /% | - | 86.6 | 81.8 | 84.6 | 84.6 |
| Specific $CO_2$ capture and conditioning work /MJe.$kg_{CO2,eq\ captured}^{-1}$ | - | 0.30 | 0.29 | 0.92 | 0.46 |
| Specific $CO_2$ emissions /$g_{CO2}$.$kWh^{-1}$ | 764 | 103 | 139 | 117 | 118 |

## 3.2    Cost performances

The cost breakdowns of the LCOE and CAC[6] of the five IGCC cases with and without $CO_2$ capture and conditioning are presented in Figure 8. It is worth noting that, in the results presented, the energy cost takes four elements into account: 1) the baseline energy cost of the power plant without capture ("energy cost without CCS"); 2) the energy penalty cost linked to the WGS ("energy penalty WGS"); 3) the energy penalty cost associated with the losses of hydrogen in the $CO_2$ product and the hydrogen content limitation for the gas turbine ("energy penalty $H_2$ losses and gas turbine"); 4) the energy penalty associated with the $CO_2$ capture and conditioning units ("energy penalty $CO_2$ capture and conditioning").

Overall, the evaluation shows that the IGCC plant with $CO_2$ capture results in LCOEs between 91 and 120 €.$MWh^{-1}$, leading therefore to a cost increase of at least 40% compared to the IGCC power plant without capture (65 €.$MWh^{-1}$). These electricity costs result in CAC from 42 to 84 €.$t_{CO2,avoided}^{-1}$. As can be seen from Figure 8, the energy cost related to the loss in net power output is the main contributor to the increase in LCOE and therefore the main contributor to the CAC. Indeed, the energy cost accounts for 68-85% of the LCOE increase, depending on the $CO_2$ capture technology employed. The remaining cost items make rather similar contributions to the increase in costs across all the cases, although higher $CO_2$ capture and conditioning investment costs are observed.

The Rectisol-based $CO_2$ capture process, which is the most mature technology, used as reference technology in this work, results in an electricity cost of 96 €.$MWh^{-1}$ and a CAC of 47 €.$t_{CO2,avoided}^{-1}$, while the low-temperature capture results in an LCOE of 91 €.$MWh^{-1}$ and a CAC of 42 €.$t_{CO2,avoided}^{-1}$. The low-temperature capture process is therefore slightly cheaper than the Rectisol-based $CO_2$ capture (4% in terms of LCOE and 6% in term of CAC). Indeed, in addition of being slightly more energy efficiency compared to the Rectisol-based process, the low-temperature technology also results in lower $CO_2$ capture investment cost (despite the higher contingency costs included), as well as lower variable operating costs. Regarding the membrane-based capture processes, both of the processes based on membranes A and B result in significantly higher LCOEs and CACs than the reference capture technology. In fact, the membrane process based on membrane A leads to a LCOE and CAC of 120 €.$MWh^{-1}$ and 84 €.$t_{CO2,avoided}^{-1}$ respectively, while costs of 99 €.$MWh^{-1}$ and 53 €.$t_{CO2,avoided}^{-1}$ are achieved when membrane B is employed. The membrane-based capture processes therefore result in CACs for membranes A and B respectively that are 80 and 13 % higher than for the reference capture technology. The main reasons for these significant cost increases for the membranes processes are both the lower net power outputs of the IGCC plant with membrane-based capture and, to a lower extent, the higher $CO_2$ capture and conditioning investments required, due to the high membrane area and compression work involved. Furthermore, despite the low contribution of the $CO_2$ capture and conditioning investment costs to the $CO_2$ avoided cost, it is worth noting that significantly higher membrane costs may arise during early phases of deployment [54], thus making these two membrane options even less attractive.

Based on the obtained costs, both the low-temperature and Rectisol-based capture technologies appear to be the most cost-effective options for $CO_2$ capture from the IGCC plant, given their very similar costs. While the low-temperature capture technology leads to slightly lower costs and initial investments, the Rectisol-based process is more mature, is slightly more efficient, and has the advantage of existing experience at the Vřesová plant for syngas desulphurisation. Thus, while Rectisol-based capture is the most likely scenario for implementation at least in the near future, further industrial-scale testing needs to be carried out to bring low-temperature capture technology closer to demonstration maturity and reduce costs.

---

[6] Here only the cost of $CO_2$ capture and conditioning is included, while the costs associated with $CO_2$ transport and storage will be included when discussing the entire chain in section 4.3.
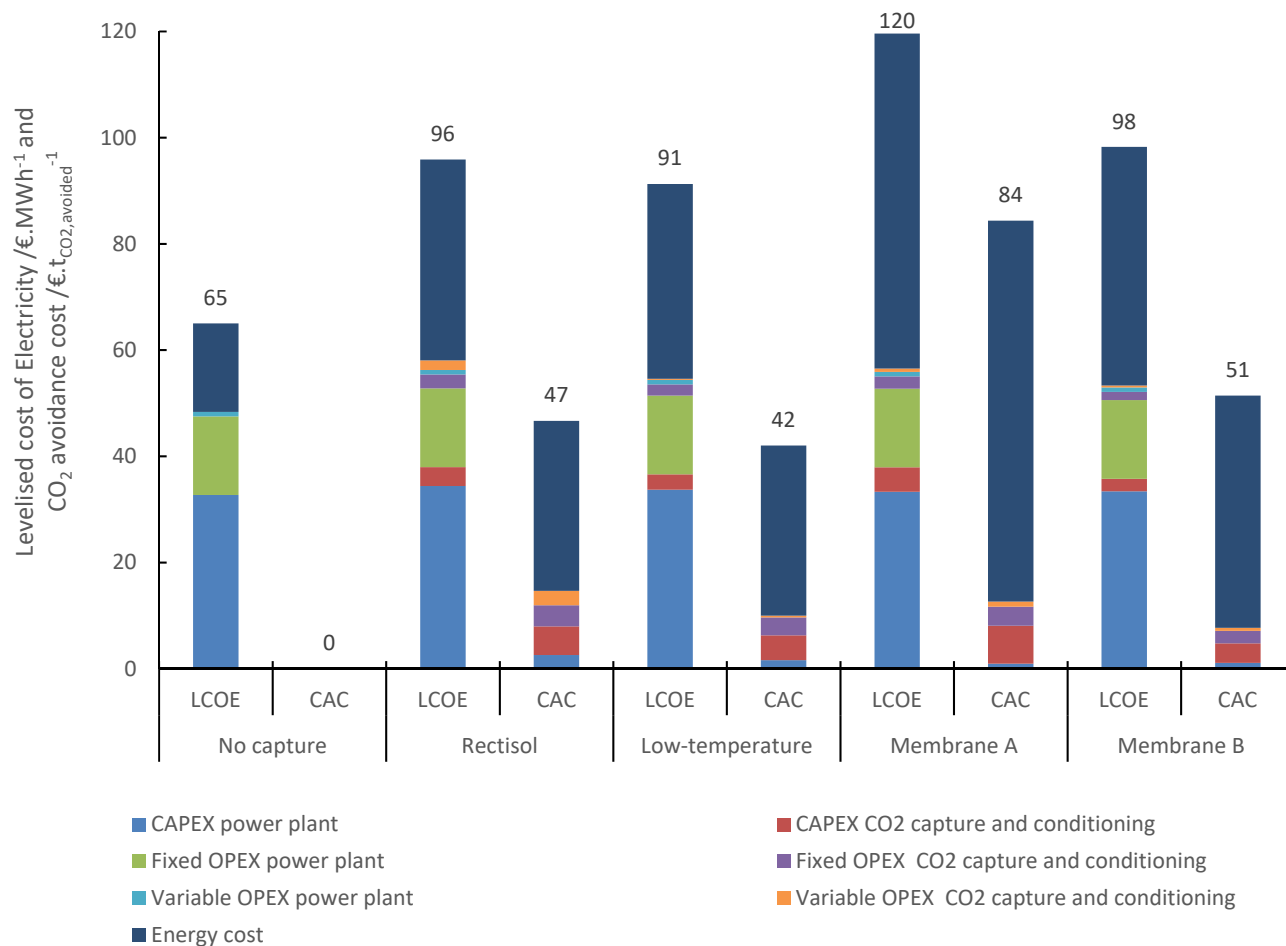
Figure 8: LCOE and CAC of IGCC plant with and without $CO_2$ capture

As discussed above, the cost estimates presented here take into account the level of maturity of the different $CO_2$ capture technologies. However, there are inherent uncertainties regarding the process and project contingencies to be assumed during the cost assessments, and it is therefore important to quantify the impact of these uncertainties on the cost and technology comparisons. For this reason, the CAC of all four capture technologies are evaluated taking two additional maturity scenarios into consideration. The first assumes that the $CO_2$ capture technologies are commercially mature technology and that both process and project contingencies related to technology maturity are thus zero for the $CO_2$ capture units. The second scenario assumes that the technical and cost modelling of the $CO_2$ capture are based on a technology at the bench-scale level and the process and project contingencies are assumed to be 50 and 25% respectively for the $CO_2$ capture units [46, 47].

The CAC of these two maturity scenarios and the base case maturity scenario are shown in Figure 9. The results show that the maturity levels have a relatively limited impact on the CAC, within ±8% of the base case, depending on the technology. This low influence is directly due to the limited contribution of the $CO_2$ capture investment cost to the CAC, especially for the low-temperature and Rectisol capture technologies. Therefore, the results presented in Figure 9 show that the uncertainties on the technology maturity level will not have a significant impact on the cost-competeveness of the low-temperature and Rectisol capture technologies.
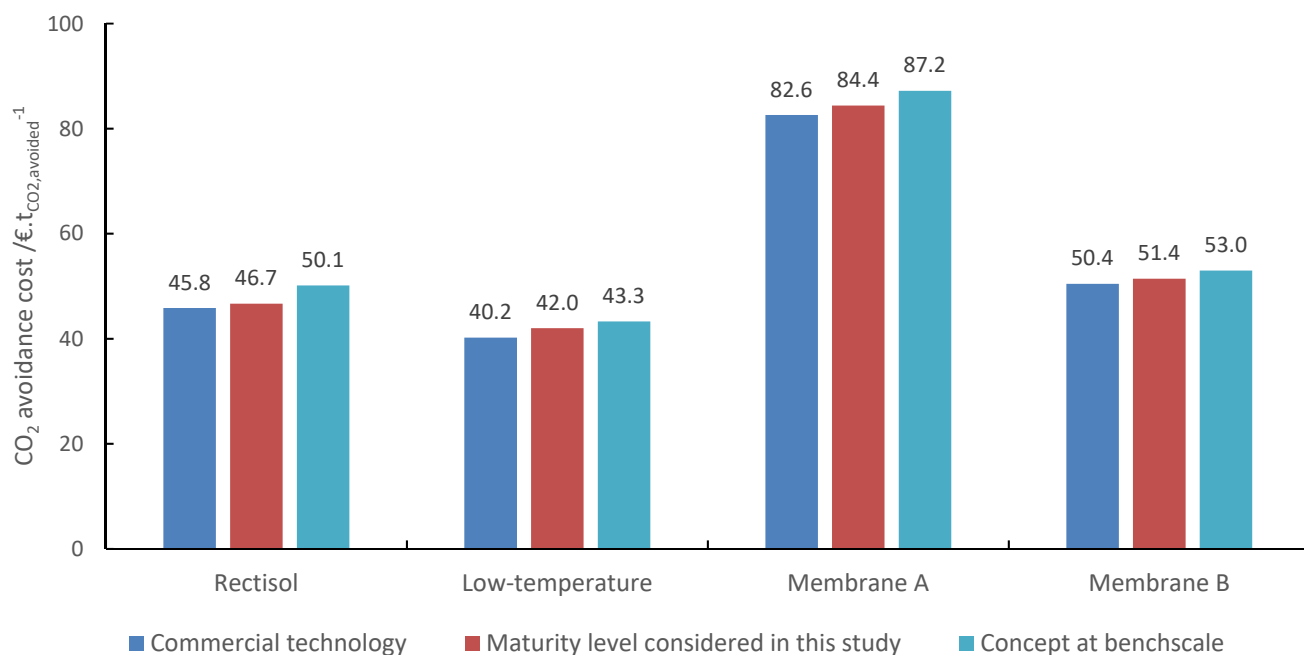
Figure 9: Impact of the assumed technology maturity on the CAC

## 4  Discussions

### 4.1  Impact of $CO_2$ Capture Ratio

The importance of the $CO_2$ capture ratio (CCR) on the energy and cost performances of $CO_2$ capture technologies, and therefore the potential of partial capture, has been emphasised in the literature [31, 55] and CCR may impact the different capture technologies differently. Indeed, solvent-based captures have been shown to operate best at CCRs of 90% and above, while lower CCRs, for example, have been shown to be able to significantly reduce $CO_2$ capture costs for post-combustion membrane-based capture [31]. It is therefore important to investigate the impact of the $CO_2$ capture ratio on the performance of each technology and the selection of the optimal capture technology.

Figure 10 presents the CAC evaluations of the power plant with the considered capture technologies for CCRs ranging from 50 to 90%, while the corresponding LCOE and CAC values are shown in Table 9. The evaluations show that the CAC increases when the CCR decreases for both the Rectisol and the low-temperature based capture processes. Indeed, the CAC of Rectisol capture increases by 19% when CCR falls from 85 to 60%. Meanwhile, for the low-temperature based capture, the CAC increases by 13% when the CCR falls from 85 to 50%. However, in the case of the membrane-based capture, it appears that there are cost-optimal CCRs around 60-75%, which result in CAC cost-reductions beyond 16 and 11%, for membranes A and B respectively. Although partial capture appears to reduce the cost of membrane-based captures and enables them to outperform Rectisol capture, low-temperature capture remains more cost-effective even when considering partial capture. Howbeit, the potential of low-temperature capture compared to Rectisol based capture increases as the CCR decreases.

Finally, it is worth noting that lower CCRs result in lower LCOEs, as $CO_2$ capture investments and energy penalties increase with the amount of $CO_2$ captured. Therefore, implementing $CO_2$ capture with CCRs lower than 85% could result in both lower cost penalty associated with the capture (lower CACs) and more cost-competitive power plants with capture (lower LCOEs). Thus, the considering lower CCRs may be a key element in ensuring early implementation of $CO_2$ capture while maintaining the economic viability of the power plant.

Table 9: LCOE and CAC of the power plant with the different capture technologies depending on the $CO_2$ capture ratio

| KPIs | $CO_2$ capture ratio /% | 50 | 60 | 75 | 85 |
|---|---|---|---|---|---|
| | Rectisol | - | 91 | 96 | 97 |
| LCOE /€.MWh⁻¹ | Low-temperature | 83 | - | - | 91 |
| | Capture process based on membrane A | 95 | 98 | 108 | 120 |

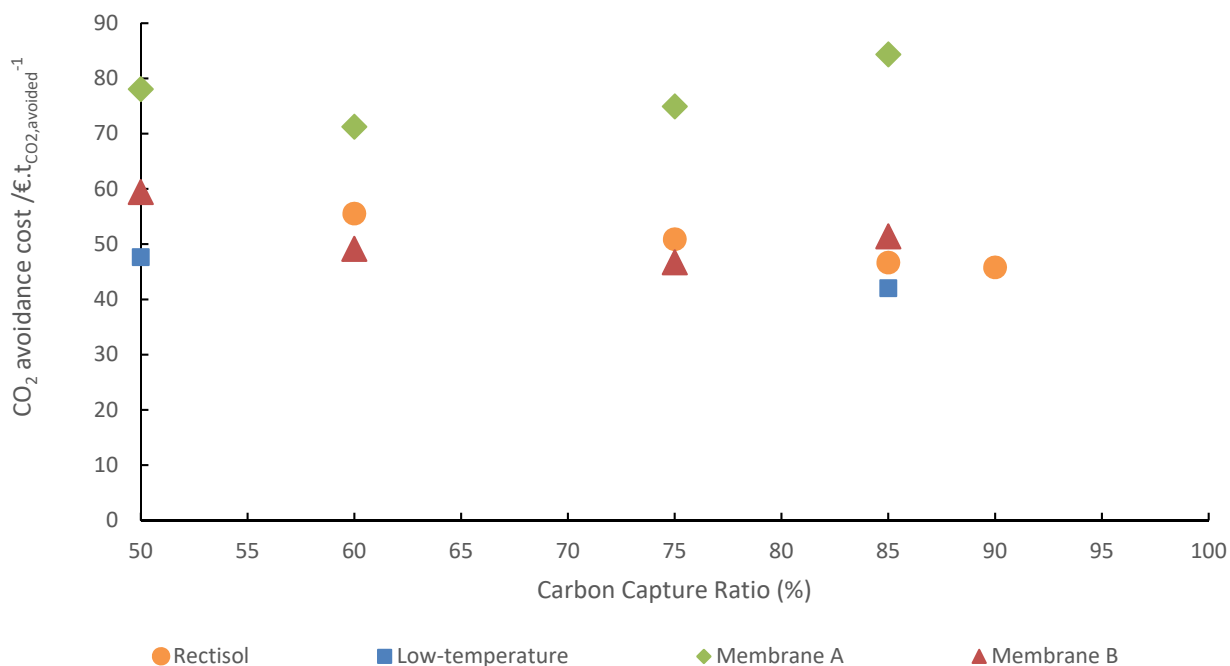| | | | | | |
|---|---|---|---|---|---|
| | Capture process based on membrane B | 88 | 87 | 92 | 99 |
| CAC /€.t$_{CO2,avoided}^{-1}$ | Rectisol | - | 56 | 51 | 47 |
| | Low-temperature | 48 | - | - | 42 |
| | Capture process based on membrane A | 78 | 71 | 75 | 84 |
| | Capture process based on membrane B | 59 | 49 | 47 | 53 |



Figure 10: CAC of the different capture technologies depending on the CO$_2$ capture ratio

## 4.2    Potential of CO$_2$-selective membrane

As discussed above, the CO$_2$-selective membranes considered result in CO$_2$ capture processes with high energy and cost penalties. To assess more systematically the potential of polymeric CO$_2$-selective membranes for pre-combustion CO$_2$ capture from an IGCC power plant, the impact of membrane properties on the CAC shall be further investigated. As previously done for post-combustion capture [30, 32], the membrane numerical model used in the present study is also used to optimise and assess the levelised cost of electricity of the power plant with membrane-based capture for a wide range of membrane properties (selectivity and permeance). Selectivity up to 160 and permeances up to 10 m$^3_{(STP)}$.m$^{-2}$.h$^{-1}$.bar$^{-1}$ are here considered to represent both current and possible future membrane properties.

The CACs obtained are plotted in Figure 11 as function of the membrane permeance and selectivity in the form of a contour diagram. The results show that CACs similar to those of the Rectisol-based process can only be achieved with high selectivities or with high permeances for selectivities between 50 and 100. This emphasises the importance of developing high-potential materials (such as fixed-site carrier membranes, metal organic framework membranes and mixed matrix membranes) and advanced process configurations (recycle, sweep, etc) for CO$_2$-selective membranes to become competitive with Rectisol-based and low-temperature based capture processes. While the development of such material until the commercial stage may require significant cost and long time, the results presented in Figure 11 could be used to guide the development of such membranes and therefore help faster and more cost-efficient technology development [32].

Finally, it is worth noting that the potential of H$_2$-selective membranes [56], like palladium and ceramic membranes, and WGS membrane reactor [57]  could result in better performances than CO$_2$-selective membranes and should therefore be further investigated.
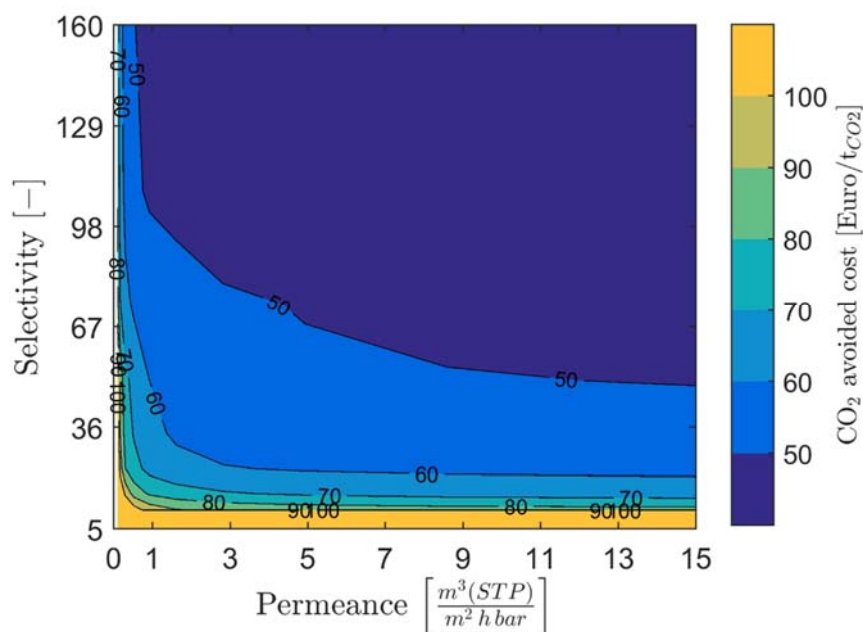
15

Figure 11: CAC contour diagram of $CO_2$-selective membrane-based capture in function of the membrane properties

## 4.3 Whole chain perspective

Finally, to provide support for a financial decision regarding the potential implementation of CCS from the considered IGCC, the cost of the whole CCS chain ($CO_2$ capture, transport and storage) needs to be evaluated.

The CCS chain considered to perform the whole chain cost assessment is defined as follows. The $CO_2$ capture technology considered for the whole CCS chain evaluation is assumed to be the Rectisol-based process. Indeed, although the low-temperature capture technology leads to slightly lower costs, the Rectisol-based capture is more mature and has the advantage of being already in use at the plant for sulphur removal. Several combinations of transport methods and storage site scenarios were evaluated and discussed for the Vřesová plant in detail previously [58]. Here, the storage scenario selected is a saline aquifer reservoir located in the Zatec Basin (Czech Republic). In addition to low storage cost (estimated at around 3.5 €.$t_{CO2,injected}^{-1}$ [58]), this potential storage site also presents the advantage of avoiding legal uncertainties around transnational transport of $CO_2$ [59]. In this case, the $CO_2$ is transported by pipeline[7] over a distance of approximately 23 km [58].

Once the whole CCS chain is included, as shown in Figure 12, the LCOE is estimated to be 101 €.MWh[-1], which corresponds to an increase of 56% compared to the IGCC power plant without capture (65 €.MWh[-1]). This increase results in a CAC of 54 €.$t_{CO2, avoided}^{-1}$. Adding $CO_2$ transport and storage to the previous estimates leads therefore to limited increases (approximately 5 €.MWh[-1] and 7.4 €.$t_{CO2,avoided}^{-1}$ for respectively the LCOE and the CAC), and the $CO_2$ capture and conditioning represent 86% of the CAC of the whole chain. This limited contribution from the $CO_2$ transport and storage is due to the short transport distance involved and the onshore storage[8] [60]. While the cost of the whole CCS chain is relatively low for a full CCS chain [61], it is important to note that these values are substantially higher than the current European carbon price. Therefore, if CCS from the Vřesová power plant is to be implemented to reduce the Czech Republic's $CO_2$ emissions, national and/or European financial support will be necessary to maintain the economic viability of the power plant with CCS.

---

[7] It is worth noting that train-based transport was also considered and deemed as not cost attractive in this case.
[8] Onshore $CO_2$ storage has been demonstrated to be significantly cheaper than offshore storage.
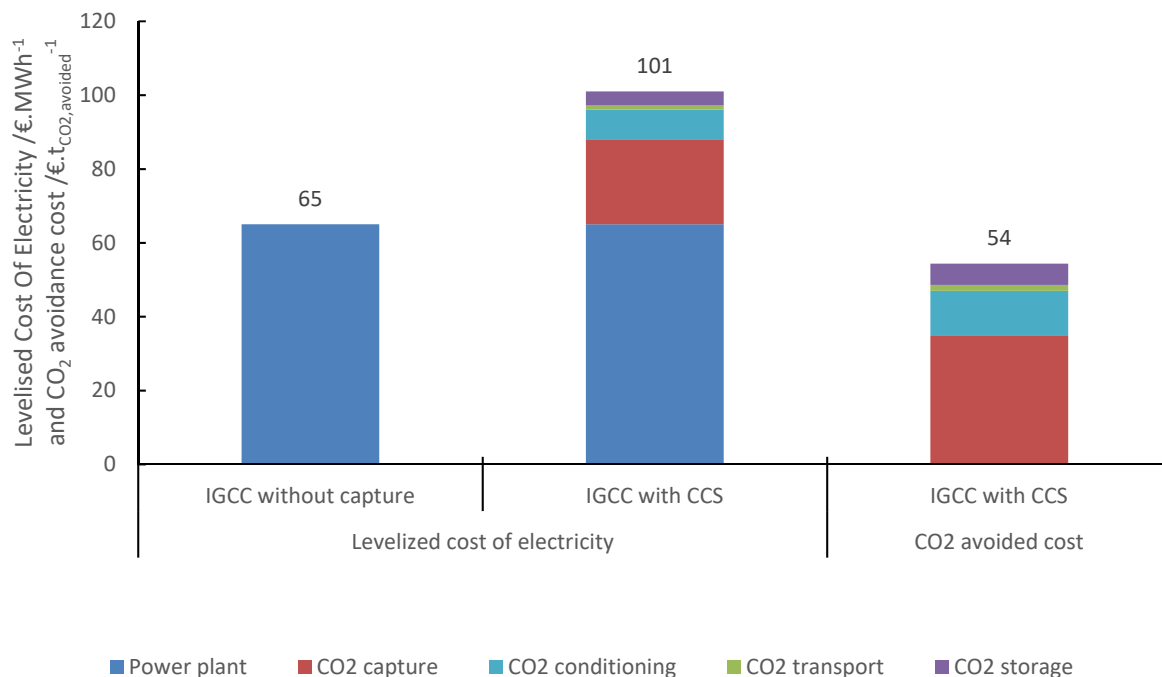
Figure 12: LCOE and CAC of the IGCC power plant with and without CCS

## 5    Conclusions

This paper compares the techno-economic performances of three technologies for $CO_2$ capture from a lignite-based IGCC power plant located in the Czech Republic: 1) physical absorption with a Rectisol-based process 2) Polymeric $CO_2$-selective membrane-based capture 3) Low-temperature capture.

For a $CO_2$ capture ratio of 85%, the evaluations show that the IGCC plant with $CO_2$ capture results in an LCOE between 91 and 120 €.MWh$^{-1}$, depending on the capture technology employed, compared to 65 €.MWh$^{-1}$ for the power plant without capture. This results in CACs that range from 42 to 84 €.t$_{CO2,avoided}$$^{-1}$, mainly due to the reduction in net power output. From both energy and cost points of view, the low-temperature and Rectisol-based $CO_2$ captures appear to be the most efficient capture technologies with CACs of 42 and 44 €.t$_{CO2,avoided}$$^{-1}$ respectively, while the avoidance costs of membrane-based capture lie beyond 53 €.t$_{CO2,avoided}$$^{-1}$. Due to the relatively low contribution of the $CO_2$ capture investment cost in the CAC, the uncertainties on the level of technological maturity, which is taken into account through process and project contingencies, do not modify the cost-competitiveness of the low-temperature and Rectisol capture technologies

Furthermore, the impact of the $CO_2$ capture ratio on the cost performances of the IGCC with the different capture technologies is also evaluated. The cost assessment shows that lower CCRs increase the CAC for the low-temperature capture and especially the Rectisol-based capture, while a cost-optimal CCR is observed around 60-75% for the $CO_2$-selective membranes-based capture. Overall, the potential of the low-temperature capture compared to the other capture technologies increases at low CCRs. Even though lower CCRs result in higher CACs, accepting lower CCRs could be a key element in ensuring early implementation of $CO_2$ capture while maintaining the economic viability of the power plant, as the CCS implementation weighs less on the LCOE of the plant.

To go beyond the two specific membranes considered, the impact of membrane properties on the CAC is further investigated in order to identify the range of membrane properties required for $CO_2$-selective membrane-based capture to become competitive with the reference solvent capture technology. The results show that membrane-based $CO_2$ capture has the potential to become cost-competitive with the reference Rectisol-based capture technology; however, advanced membrane process configurations (recycle, sweep, etc.) and significant efforts to improve current membrane properties will be required. The potential of $H_2$-selective membranes [56] and WGS membrane reactors [57] should also be considered in further work, the properties map in this study can be used to help the development of suitable $CO_2$-selective membranes.

Finally, to provide support for a financial decision regarding the potential CCS implementation from the considered IGCC, the cost of the whole chain is evaluated considering pipeline transport to a saline aquifer storage located in the Zatec Basin (Czech Republic). Once the whole CCS chain included, the LCOE is estimated to 101 €.MWh$^{-1}$, resulting in a CAC of 54 €.t$_{CO2,avoided}$$^{-1}$, to which the costs of $CO_2$ transport and storage made only a limited contribution due to the short transport distance and the onshore storage. While these costs are relatively low for a full CCS chain, these values are substantially higher than the current carbon price of the European Emissions Trading System and further national or European financial support will be required to ensure economically viable implementation.

## Acknowledgements

## References

1.  International Energy Agency, IEA Statistics: Coal information, 2015.
2.  Bauerova L, Europe's coal curtain is complicating the climate fight. Bloomberg Business. 01.12.2015.
3.  Berstad D, Roussanaly S, Skaugen G, Anantharaman R, Nekså P, Jordal K. Energy and cost evaluation of a low-temperature $CO_2$ capture unit for IGCC plants. Energy Procedia, 2014, 63(0): 2031-2036.
4.  IEAGHG, Assessment of emerging $CO_2$ capture technologies and their potential to reduce costs, 2014/TR4, 2014.
5.  Størset S, Tangen G, Berstad D, Eliasson P, Hoff K A, Langørgen Ø, Munkejord S T, Roussanaly S, Torsæter M. Profiting from CCS innovations: A study to measure potential value creation from CCS research and development. International Journal of Greenhouse Gas Control, 2019, 83: 208-215.
6.  Chen C Rubin E. $CO_2$ control technology effects on IGCC plant performance and cost. Energy Policy, 2009, 37(3): 915-924.
7.  Klara J Plunkett J. The potential of advanced technologies to reduce carbon capture costs in future IGCC power plants. International Journal of Greenhouse Gas Control, 2010, 4(2): 112-118.
8.  Lin H, He Z, Sun Z, Kniep J, Ng A, Baker R, Merkel T. $CO_2$-selective membranes for hydrogen production and $CO_2$ capture – Part II: Techno-economic analysis. Journal of Membrane Science, 2015, 493: 794-806.
9.  Urech J, Tock L, Harkin T, Hoadley A, Maréchal F. An assessment of different solvent-based capture technologies within an IGCC–CCS power plant. Energy, 2014, 64: 268-276.
10.  Anantharaman R, Bolland O, Booth N, Dorst E V, Ekstrom C, Franco F, Macchi E, Manzolini G, Nikolic D, Pfeffer A, et al., D1.4.3 European best practice guidelines for assessment of $CO_2$ capture technologies (DECARBit Project), 2011.
11.  Zhai H Rubin E. Systems analysis of physical absorption of $CO_2$ in ionic liquids for pre-combustion carbon capture. Environmental Science & Technology, 2018, 52(8): 4996-5004.
12.  Gazzani M, Turi D, Ghoniem A, Macchi E, Manzolini G. Techno-economic assessment of two novel feeding systems for a dry-feed gasifier in an IGCC plant with pd-membranes for $CO_2$ capture. International Journal of Greenhouse Gas Control, 2014, 25: 62-78.
13.  Grainger D Hägg M-B. Techno-economic evaluation of a PVAm $CO_2$-selective membrane in an IGCC power plant with $CO_2$ capture. Fuel, 2008, 87(1): 14-24.
14.  Riboldi L Bolland O. Comprehensive analysis on the performance of an IGCC plant with a PSA process integrated for $CO_2$ capture. International Journal of Greenhouse Gas Control, 2015, 43: 57-69.
15.  Gräbner M, Morstein O, Rappold D, Günster W, Beysel G, Meyer B. Constructability study on a German reference IGCC power plant with and without $CO_2$-capture for hard coal and lignite. Energy Conversion and Management, 2010, 51(11): 2179-2187.
16.  Rubin E, Booras G, Davison J, Ekstrom C, Matuszewski M, McCoy S T, Short C, Toward a common method of the cost estimation for $CO_2$ capture and storage at fossil fuel power plants. Global CCS Institute, 2013.

17. Falk-Pedersen O, Gundersen M H, Selfors A, Svendsen P T, Carbon capture and storage at Kårstø. Norges vassdrags- og energidirektorat, 2007.

18. Garðarsdóttir S, Normann F, Skagestad R, Johnsson F. Investment costs and $CO_2$ reduction potential of carbon capture from industrial plants – A Swedish case study. International Journal of Greenhouse Gas Control, 2018, 76: 111-124.

19. Roussanaly S, Aasen A, Anantharaman R, Danielsen B, Jakobsen J, Heme-De-Lacotte L, Neji G, Sødal A, Wahl P E, Vrana T K, et al. Offshore power generation with carbon capture and storage to decarbonise mainland electricity and offshore oil and gas installations: A techno-economic analysis. Applied Energy, 2019, 233-234: 478-494.

20. European Technology Platform for Zero Emission Fossil Fuel Power Plants (ZEP), The costs of $CO_2$ transport, Post-demonstration CCS in the EU, 2011.

21. Roussanaly S, Jakobsen J P, Hognes E H, Brunsvold A L. Benchmarking of $CO_2$ transport technologies: Part I—Onshore pipeline and shipping between two onshore areas. International Journal of Greenhouse Gas Control, 2013, 19C.

22. Kunze C Spliethoff H. Modelling, comparison and operation experiences of entrained flow gasifier. Energy Conversion and Management, 2011, 52(5): 2135-2141.

23. Meerman J C, Knoope M M J, Ramírez A, Turkenburg W C, Faaij A P C. Technical and economic prospects of coal- and biomass-fired integrated gasification facilities equipped with CCS over time. International Journal of Greenhouse Gas Control, 2013, 16: 311-323.

24. Kapetaki Z, Ahn H, Brandani S. Detailed process simulation of pre-combustion IGCC plants using coal-slurry and dry coal gasifiers. Energy Procedia, 2013, 37: 2196-2203.

25. Padurean A, Cormos C-C, Agachi P-S. Pre-combustion carbon dioxide capture by gas–liquid absorption for integrated gasification combined cycle power plants. International Journal of Greenhouse Gas Control, 2012, 7: 1-11.

26. Park S, Lee S, Lee J, Chun S, Lee J. The quantitative evaluation of two-stage pre-combustion $CO_2$ capture processes using the physical solvents with various design parameters. Energy, 2015, 81: 47-55.

27. Sun L Smith R. Rectisol wash process simulation and analysis. Journal of Cleaner Production, 2013, 39: 321-328.

28. Li P, Wang Z, Qiao Z, Liu Y, Cao X, Li W, Wang J, Wang S. Recent developments in membranes for efficient hydrogen purification. Journal of Membrane Science, 2015, 495: 130-168.

29. Qiao Z, Wang Z, Yuan S, Wang J, Wang S. Preparation and characterization of small molecular amine modified PVAm membranes for $CO_2/H_2$ separation. Journal of Membrane Science, 2015, 475: 290-302.

30. Roussanaly S, Anantharaman R, Lindqvist K, Zhai H, Rubin E. Membrane properties required for post-combustion $CO_2$ capture at coal-fired power plants. Journal of Membrane Science, 2016, 511: 250-264.

31. Roussanaly S Anantharaman R. Cost-optimal $CO_2$ capture ratio for membrane-based capture from different $CO_2$ sources. Chemical Engineering Journal, 2017, 327: 618-628.

32. Roussanaly S, Anantharaman R, Lindqvist K, Hagen B. A new approach to the identification of high-potential materials for cost-efficient membrane-based post-combustion $CO_2$ capture. Sustainable Energy & Fuels, 2018, 2(6): 1225-1243.

33. Saltonstall C. Calculation of the membrane area required for gas separations. Journal of Membrane Science, 1987, 32(2–3): 185-193.

34. Zhai H Rubin E. Techno-economic assessment of polymer membrane systems for post-combustion carbon capture at coal-fired power plants. Environmental Science & Technology, 2013, 47(6): 3006-3014.

35. Merkel T, Lin H, Wei X, Baker R. Power plant post-combustion carbon dioxide capture: An opportunity for membranes. Journal of Membrane Science, 2010, 359(1–2): 126-139.

36. He X, Fu C, Hägg M-B. Membrane system design and process feasibility analysis for $CO_2$ capture from flue gas with a fixed-site-carrier membrane. Chemical Engineering Journal, 2015, 268: 1-9.

37. Vakharia V, Ramasubramanian K, Winston H. An experimental and modeling study of $CO_2$-selective membranes for IGCC syngas purification. Journal of Membrane Science, 2015, 488: 56-66.

38. Lin H  Freeman B. Materials selection guidelines for membranes that remove $CO_2$ from gas mixtures. Journal of Molecular Structure, 2005, 739(1): 57-74.

39. Lin H, He Z, Sun Z, Vu J, Ng A, Mohammed M, Kniep J, Merkel T, Wu T, Lambrecht R. $CO_2$-selective membranes for hydrogen production and $CO_2$ capture – Part I: Membrane development. Journal of Membrane Science, 2014, 457: 149-161.

40. Berstad D, Anantharaman R, Nekså P. Low-temperature $CO_2$ capture technologies – Applications and potential. International Journal of Refrigeration, 2013, 36(5): 1403-1416.

41. Anantharaman R, Berstad D, Roussanaly S. Techno-economic performance of a hybrid membrane-liquefaction process for post-combustion $CO_2$ capture. Energy Procedia, 2014, 61(0): 1244-1247.

42. Voldsund M, Gardarsdottir S, De Lena E, Pérez-Calvo J-F, Jamali A, Berstad D, Fu C, Romano M, Roussanaly S, Anantharaman R, et al. Comparison of technologies for $CO_2$ capture from cement production – Part 1: technical evaluation. Energies, 2019, 12(3): 559.

43. Gardarsdottir S, De Lena E, Romano M, Roussanaly S, Voldsund M, Pérez-Calvo J-F, Berstad D, Fu C, Anantharaman R, Sutter D, et al. Comparison of technologies for $CO_2$ capture from cement production – Part 2: cost analysis. Energies, 2019, 12(3): 542.

44. European Technology Platform for Zero Emission Fossil Fuel Power Plants (ZEP), The costs of $CO_2$ capture, transport and storage, post-demonstration CCS in the EU, 2011.

45. Ho M, Allinson G, Wiley D. Comparison of MEA capture cost for low $CO_2$ emissions sources in Australia. International Journal of Greenhouse Gas Control, 2011, 5(1): 49-60.

46. NETL, Quality guidelines for energy system studies: Cost estimation methodology for NETL assessments of power plant performance. DOE/NETL-2011/1455., 2011.

47. NETL, Quality guidelines for energy system studies: Technology learning curve (FOAK to NOAK). DOE/NETL-341/042211, 2012.

48. IHS, The IHS CERA European Power Capital Costs Index (EPCCI). 2013.

49. Trading Economics, Trading Economics database on Euro area inflation rate, 2011.

50. Richardson Engineering, Cost factor location manual, 2007.

51. IEAGHG, $CO_2$ Capture in Natural Gas Production by Adsorption Processes for $CO_2$ Storage, EOR and EGR, 2016.

52. Grande C A, Roussanaly S, Anantharaman R, Lindqvist K, Singh P, Kemper J. $CO_2$ capture in natural gas production by adsorption processes. Energy Procedia, 2017, 114: 2259-2264.

53. Booz & Company, Understanding lignite generation costs in Europe, 2014.

54. Zhai H. Advanced membranes and learning scale required for cost-effective post-combustion carbon capture. iScience, 2019, 13: 440-451.

55. Anantharaman R, Roussanaly S, Westman S F, Husebye J. Selection of optimal $CO_2$ capture plant capacity for better investment decisions. Energy Procedia, 2013, 37(0): 7039-7045.

56. Al-Mufachi N, Rees N, Steinberger-Wilkens R. Hydrogen selective membranes: A review of palladium-based dense metal membranes. Renewable and Sustainable Energy Reviews, 2015, 47: 540-551.

57. Di Marcoberardino G, Binotti M, Manzolini G, Viviente J, Arratibel A, Roses L, Gallucci F. Achievements of European projects on membrane reactor for hydrogen production. Journal of Cleaner Production, 2017, 161: 1442-1450.

58. Roussanaly S, Skaugen G, Aasen A, Jakobsen J, Vesely L. Techno-economic evaluation of $CO_2$ transport from a lignite-fired IGCC plant in the Czech Republic. International Journal of Greenhouse Gas Control, 2017, 65(Supplement C): 235-250.

59. Henriksen D  Ombudstvedt I. Cross-border transportation – A key to unlock full-scale CCS. Energy Procedia, 2017, 114: 7443-7458.

60. European Technology Platform for Zero Emission Fossil Fuel Power Plants (ZEP), The costs of $CO_2$ storage, post-demonstration CCS in the EU 2011.

61.     Jakobsen J, Roussanaly S, Anantharaman R. A techno-economic case study of $CO_2$ capture, transport and storage chain from a cement plant in Norway. Journal of Cleaner Production, 2017, 144: 523-539.

# 6     Appendix: Further details on results of the process modelling

Further details on the results of the process modelling in the base case (~85% $CO_2$ capture) are presented for each $CO_2$ capture technology considered in this study. These results include stream characteristics as well as equipment power and cooling duty.

## 6.1     Rectisol-based $CO_2$ capture process

A more detailed process flow diagram of the Rectisol-based $CO_2$ capture process is presented in Figure 13, corresponding stream characteristics and power balance are presented in respectively Tables 10 and 11.



**Figure 13: Process flow diagram of the Rectisol-based $CO_2$ capture process including stream and equipment tags**

**Table 10: Stream characteristics along the Rectisol-based $CO_2$ capture process**

| Stream no. | 1 | 2 | 3 | 4 | 5 | 6 | 7 | 8 | 9 | 10 | 11 | 12 | 13 | 14 | 15 | 16 | 17 | 18 | 19 | 20 | 21 | 22 | 23 | 24 | 25 |
|---|---|---|---|---|---|---|---|---|---|---|---|---|---|---|---|---|---|---|---|---|---|---|---|---|---|
| Molar Flow /$10^3$ kmol.h$^{-1}$ | 11.99 | 12.02 | 32.49 | 32.37 | 0.95 | 31.42 | 2.22 | 29.20 | 1.02 | 4.20 | 28.18 | 28.18 | 28.18 | 0.13 | 0.13 | 0.13 | 0.10 | 0.01 | 0.09 | 0.00 | 0.08 | 0.03 | 0.11 | 0.11 | 7.81 |
| Mass Flow /kg.s$^{-1}$ | 67.93 | 68.22 | 304.5 | 303.3 | 11.28 | 292.0 | 27.12 | 264.9 | 12.42 | 50.95 | 252.5 | 252.5 | 252.5 | 1.20 | 1.20 | 1.20 | 0.91 | 0.13 | 0.77 | 0.02 | 0.75 | 0.24 | 0.99 | 0.99 | 17.19 |
| Temperature /°C | 6.6 | 3.4 | -2.9 | -2.9 | -5.4 | -5.4 | -13.5 | -13.5 | -17.5 | 30.0 | -17.5 | -17.0 | -20.0 | -2.9 | -2.8 | -20.0 | 4.2 | 6.8 | 122.8 | 144.2 | 93.7 | 20.0 | -20.0 | -19.7 | -18.4 |
| Pressure /bar | 27.9 | 27.0 | 26.6 | 26.6 | 8.0 | 8.0 | 3.0 | 3.0 | 1.0 | 110 | 1.0 | 30.0 | 29.9 | 26.6 | 31.0 | 31.0 | 27.0 | 7.0 | 7.0 | 4.0 | 3.0 | 30.0 | 3.0 | 29.0 | 26.5 |
| Molar composition /%mol | | | | | | | | | | | | | | | | | | | | | | | | | |
| H$_2$ | 53.5 | 53.3 | 0.1 | 0.1 | 2.0 | 0 | 0 | 0 | 0 | 0.4 | 0 | 0 | 0 | 0.1 | 0.1 | 0.1 | 0.1 | 0.5 | 0 | 0 | 0 | 0 | 0 | 0 | 81.8 |
| CO$_2$ | 38.7 | 38.7 | 14.3 | 14.3 | 95.4 | 11.9 | 99.4 | 5.2 | 98.9 | 98.4 | 1.8 | 1.8 | 1.8 | 14.3 | 14.3 | 14.3 | 10.8 | 97.9 | 0 | 0 | 0 | 0 | 0 | 0 | 6.5 |
| N$_2$ | 5.9 | 5.9 | 0.1 | 0.1 | 1.8 | 0 | 0.1 | 0 | 0 | 0.4 | 0 | 0 | 0 | 0.1 | 0.1 | 0.1 | 0 | 0.4 | 0 | 0 | 0 | 0 | 0 | 0 | 8.8 |
| CO | 1.1 | 1.1 | 0 | 0 | 0.1 | 0 | 0 | 0 | 0 | 0 | 0 | 0 | 0 | 0 | 0 | 0 | 0 | 0 | 0 | 0 | 0 | 0 | 0 | 0 | 1.7 |
| Ar | 0.8 | 0.8 | 0 | 0 | 0.3 | 0 | 0 | 0 | 0 | 0.1 | 0 | 0 | 0 | 0 | 0 | 0 | 0 | 0.1 | 0 | 0 | 0 | 0 | 0 | 0 | 1.2 |
| H$_2$O | 0 | 0 | 0 | 0 | 0 | 0 | 0 | 0 | 0 | 0.0 | 0 | 0 | 0 | 0 | 0 | 0 | 4.2 | 0 | 4.7 | 99.8 | 0 | 0 | 0 | 0 | 0 |
| MeOH | 0 | 0.2 | 85.5 | 85.5 | 0.3 | 88.1 | 0.5 | 94.7 | 1.0 | 0.6 | 98.1 | 98.1 | 98.1 | 85.5 | 85.5 | 85.5 | 84.9 | 0.8 | 95.3 | 0.2 | 100 | 100 | 100 | 100 | 0 |

**Table 11: Power balance of the Rectisol-based $CO_2$ capture process**

| | Power requirement /MW |
|---|---|
| Solvent pump 1 (P1) | 0.004 |
| Solvent pump 2 (P2) | 1.18 |
| Solvent pump 3 (P3) | 0.001 |
| CO$_2$ compression stage 1 (C1) | 1.00 |
| CO$_2$ compression stage 2 (C2) | 2.85 |
| CO$_2$ compression stage 3 (C3) | 5.26 |
| CO$_2$ compression stage 4 (C4) | 4.80 |
| Total | 15.09 |

## 6.2 Low-temperature based $CO_2$ process

A more detailed process flow diagram of the low-temperature based $CO_2$ capture process is presented in Figure 14, corresponding stream characteristics and power balance are presented in respectively Tables 12 and 13.
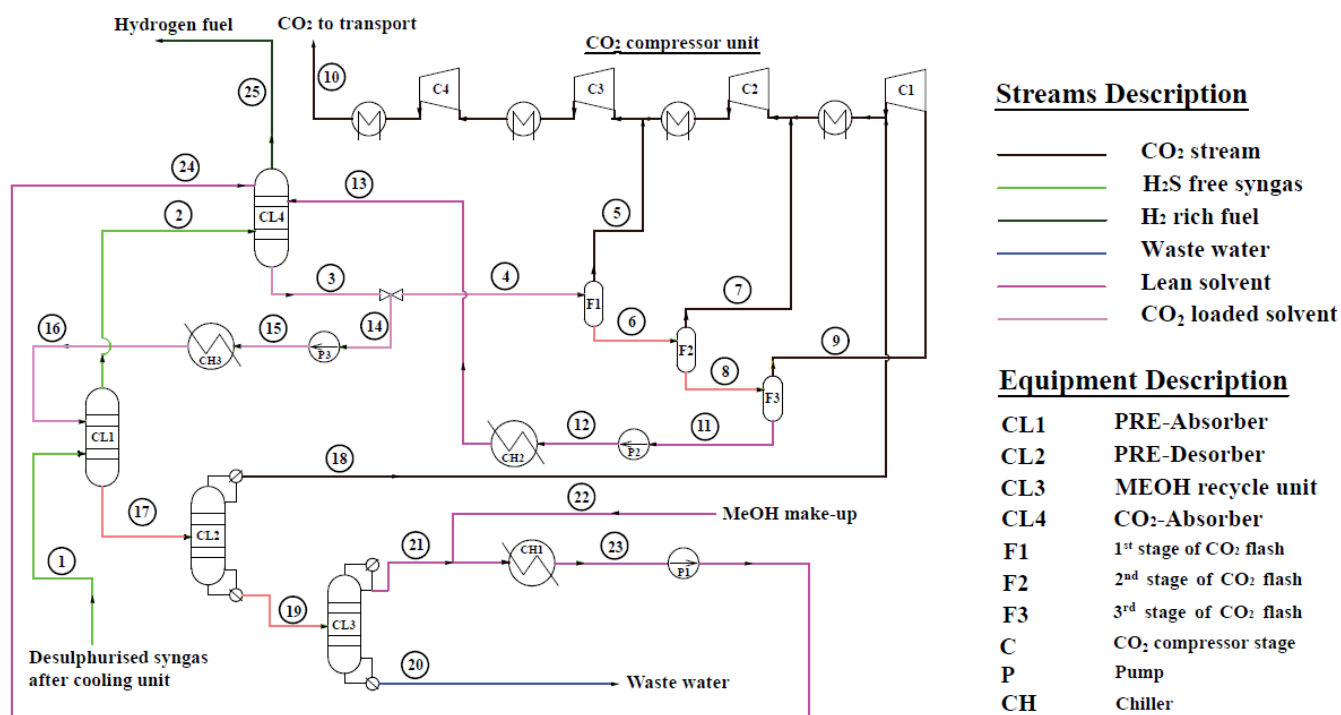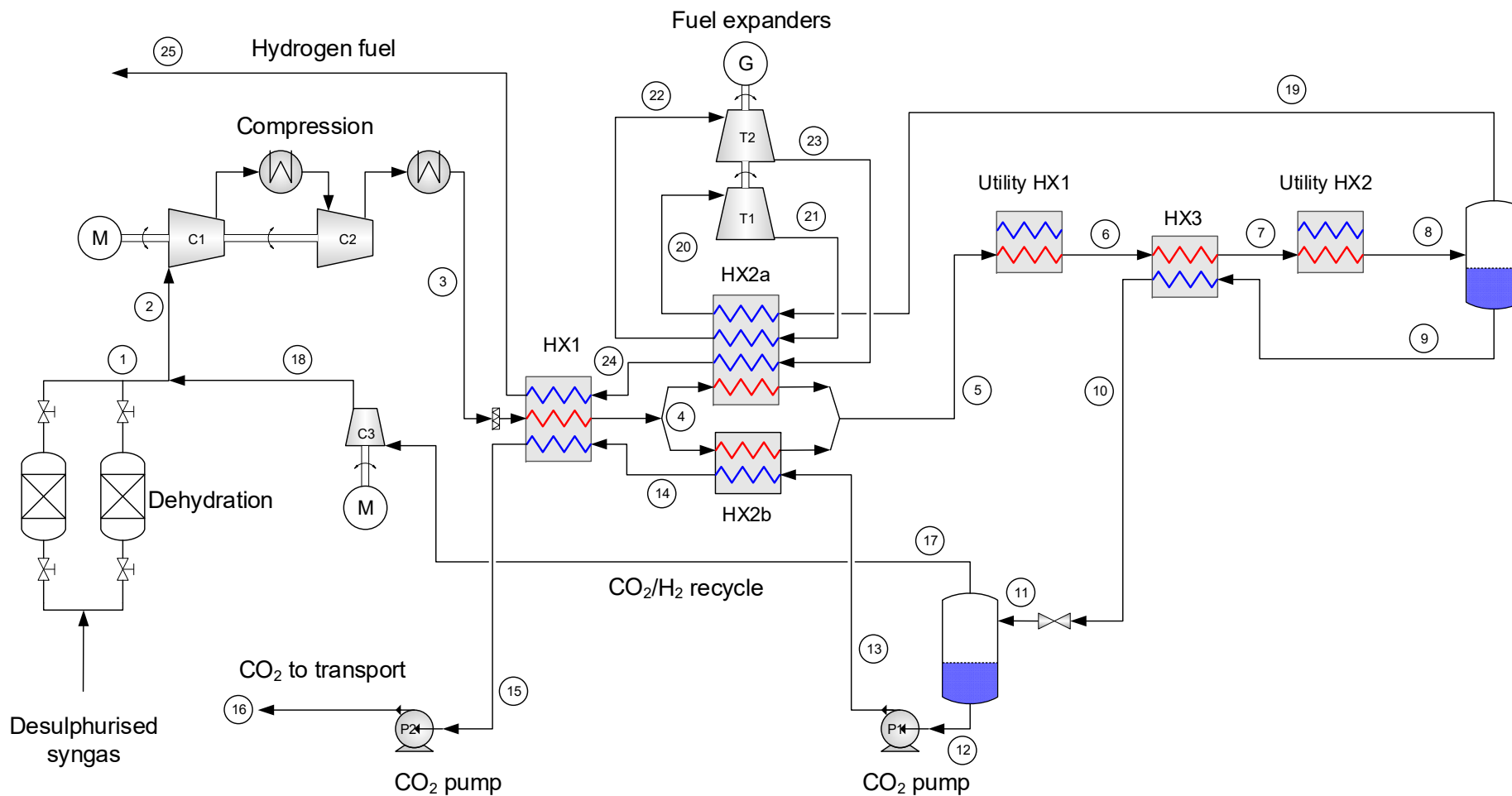


**Figure 14: Process flow diagram of the low-temperature based $CO_2$ capture process including stream and equipment tags**

**Table 12: Stream characteristics along the low-temperature based $CO_2$ capture process**

| Stream no. | 1 | 2 | 3 | 4 | 5 | 6 | 7 | 8 | 9 | 10 | 11 | 12 | 13 | 14 | 15 | 16 | 17 | 18 | 19 | 20 | 21 | 22 | 23 | 24 | 25 |
|---|---|---|---|---|---|---|---|---|---|---|---|---|---|---|---|---|---|---|---|---|---|---|---|---|---|
| Molar Flow /$10^3$ kmol.h$^{-1}$ | 12.00 | 12.57 | 12.57 | 12.57 | 12.57 | 12.57 | 12.57 | 12.57 | 4.48 | 4.48 | 4.48 | 3.92 | 3.92 | 3.92 | 3.92 | 3.92 | 0.56 | 0.56 | 8.09 | 8.09 | 8.09 | 8.09 | 8.09 | 8.09 | 8.09 |
| Mass Flow /kg.s$^{-1}$ | 67.98 | 73.38 | 73.38 | 73.38 | 73.38 | 73.38 | 73.38 | 73.38 | 53.19 | 53.19 | 53.19 | 47.82 | 47.82 | 47.82 | 47.82 | 47.82 | 5.37 | 5.37 | 20.19 | 20.19 | 20.19 | 20.19 | 20.19 | 20.19 | 20.19 |
| Temperature /°C | 30.0 | 30.6 | 30.0 | 6.9 | -30.1 | -39.2 | -42.8 | -55.2 | -55.2 | -42.2 | -55.2 | -55.2 | -51.1 | -8.9 | 1.5 | 7.5 | -55.2 | 43.5 | -55.2 | 0.9 | -55.6 | 0.9 | -55.2 | -29.0 | 1.5 |
| Pressure /bar | 27.7 | 27.7 | 104.7 | 104.4 | 104.1 | 103.8 | 103.5 | 103.2 | 103.2 | 102.2 | 8.1 | 8.1 | 90.0 | 89.0 | 88.0 | 150.0 | 8.1 | 28.0 | 103.2 | 102.9 | 40.4 | 40.1 | 15.6 | 15.3 | 15.0 |
| Molar composition /%mol | | | | | | | | | | | | | | | | | | | | | | | | | |
| H$_2$ | 53.50 | 51.94 | 51.94 | 51.94 | 51.94 | 51.94 | 51.94 | 51.94 | 2.43 | 2.43 | 2.43 | 0.05 | 0.05 | 0.05 | 0.05 | 0.05 | 18.97 | 18.97 | 79.36 | 79.36 | 79.36 | 79.36 | 79.36 | 79.36 | 79.36 |
| CO$_2$ | 38.70 | 40.03 | 40.03 | 40.03 | 40.03 | 40.03 | 40.03 | 40.03 | 95.75 | 95.75 | 95.75 | 99.73 | 99.73 | 99.73 | 99.73 | 99.73 | 68.15 | 68.15 | 9.17 | 9.17 | 9.17 | 9.17 | 9.17 | 9.17 | 9.17 |
| N$_2$ | 5.90 | 6.03 | 6.03 | 6.03 | 6.03 | 6.03 | 6.03 | 6.03 | 1.21 | 1.21 | 1.21 | 0.12 | 0.12 | 0.12 | 0.12 | 0.12 | 8.77 | 8.77 | 8.70 | 8.70 | 8.70 | 8.70 | 8.70 | 8.70 | 8.70 |
| CO | 1.10 | 1.13 | 1.13 | 1.13 | 1.13 | 1.13 | 1.13 | 1.13 | 0.25 | 0.25 | 0.25 | 0.03 | 0.03 | 0.03 | 0.03 | 0.03 | 1.81 | 1.81 | 1.62 | 1.62 | 1.62 | 1.62 | 1.62 | 1.62 | 1.62 |
| Ar | 0.80 | 0.87 | 0.87 | 0.87 | 0.87 | 0.87 | 0.87 | 0.87 | 0.35 | 0.35 | 0.35 | 0.07 | 0.07 | 0.07 | 0.07 | 0.07 | 2.31 | 2.31 | 1.15 | 1.15 | 1.15 | 1.15 | 1.15 | 1.15 | 1.15 |

**Table 13: Electrical power balance of the low-temperature based $CO_2$ capture process**

| | Power Requirement /MW |
|---|---|
| 1st compressor stage (C1) | 7.39 |
| 2nd compressor stage (C2) | 7.34 |
| Recirculation compressor (C3) | 0.48 |
| Liquid CO2 pump (P1) | 0.45 |
| End-product CO2 pump (P2) | 0.41 |
| H2 fuel turbine 1 (T1) | -3.21 |
| H2 fuel turbine 2 (T2) | -3.23 |
| Auxiliary refrigeration for Utility HX1 | 1.70 |
| Auxiliary refrigeration for Utility HX2 | 2.56 |
| Total | 13.90 |

## 6.3 CO₂-selective membrane-based CO₂ capture process

A more detailed process flow diagram of the $CO_2$ capture processes based on the $CO_2$-selective membranes A and B are respectively presented in Figures 15 and 16. For the process based on membrane A, the corresponding stream characteristics and power balance are presented in respectively Tables 15 and 16, while this information is available in Tables 17 and 18 for the process based on membrane B.
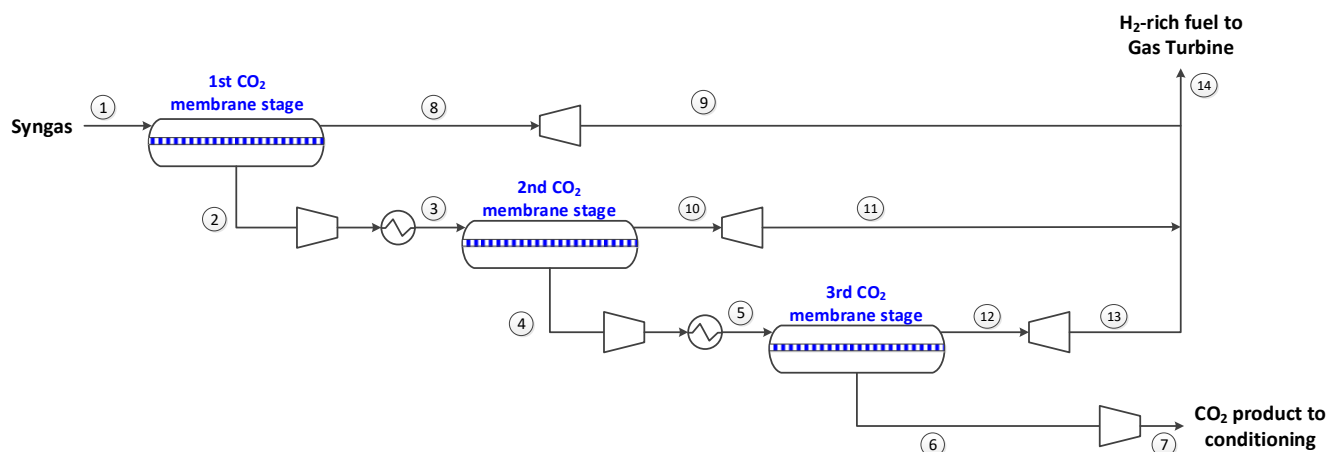


**Figure 15: Process flow diagram of the CO₂ capture process based on the CO₂-selective membrane A including stream tags**

**Table 14: Stream characteristics along the CO₂ capture process based on the CO₂-selective membrane A**

| Stream no. | 1 | 2 | 3 | 4 | 5 | 6 | 7 | 8 | 9 | 10 | 11 | 12 | 13 | 14 |
|---|---|---|---|---|---|---|---|---|---|---|---|---|---|---|
| Molar Flow /10³ kmol.h⁻¹ | 12.03 | 6.84 | 6.84 | 5.00 | 5.00 | 4.27 | 4.27 | 5.04 | 5.04 | 1.80 | 1.80 | 0.72 | 0.72 | 7.57 |
| Mass Flow /kg.s⁻¹ | 68.00 | 58.09 | 58.09 | 53.17 | 53.17 | 49.96 | 49.96 | 9.91 | 9.91 | 4.92 | 4.92 | 3.21 | 3.21 | 18.05 |
| Temperature /°C | 30.0 | 30.0 | 30.0 | 30.0 | 30.0 | 30.0 | 30.0 | 30.0 | -15.9 | 30.0 | -15.8 | 30.0 | -14.1 | -15.7 |
| Pressure /bar | 28.0 | 1.6 | 28.3 | 2.1 | 28.3 | 1.8 | 150.0 | 28.0 | 14.0 | 28.3 | 14.0 | 28.3 | 14.0 | 14.0 |
| Molar composition /%mol | | | | | | | | | | | | | | |
| H₂ | 53.41 | 30.32 | 30.32 | 12.94 | 12.94 | 4.35 | 4.35 | 83.40 | 83.40 | 77.15 | 77.15 | 63.11 | 63.11 | 79.98 |
| CO₂ | 38.64 | 65.17 | 65.17 | 85.14 | 85.14 | 95.00 | 95.00 | 4.19 | 4.19 | 11.36 | 11.36 | 27.49 | 27.49 | 8.12 |
| N₂ | 5.89 | 3.34 | 3.34 | 1.43 | 1.43 | 0.48 | 0.48 | 9.20 | 9.20 | 8.51 | 8.51 | 6.96 | 6.96 | 8.82 |
| CO | 1.08 | 0.61 | 0.61 | 0.26 | 0.26 | 0.09 | 0.09 | 1.69 | 1.69 | 1.56 | 1.56 | 1.28 | 1.28 | 1.62 |
| Ar | 0.80 | 0.45 | 0.45 | 0.19 | 0.19 | 0.07 | 0.07 | 1.25 | 1.25 | 1.16 | 1.16 | 0.95 | 0.95 | 1.20 |
| Other* | 0.18 | 0.10 | 0.10 | 0.04 | 0.04 | 0.01 | 0.01 | 0.28 | 0.28 | 0.26 | 0.26 | 0.21 | 0.21 | 0.27 |

\* $H_2O$, HCL, COS, $CH_4$, etc.

**Table 15: Electrical power balance and membrane area of the CO₂ capture process based on the CO₂-selective membrane A**

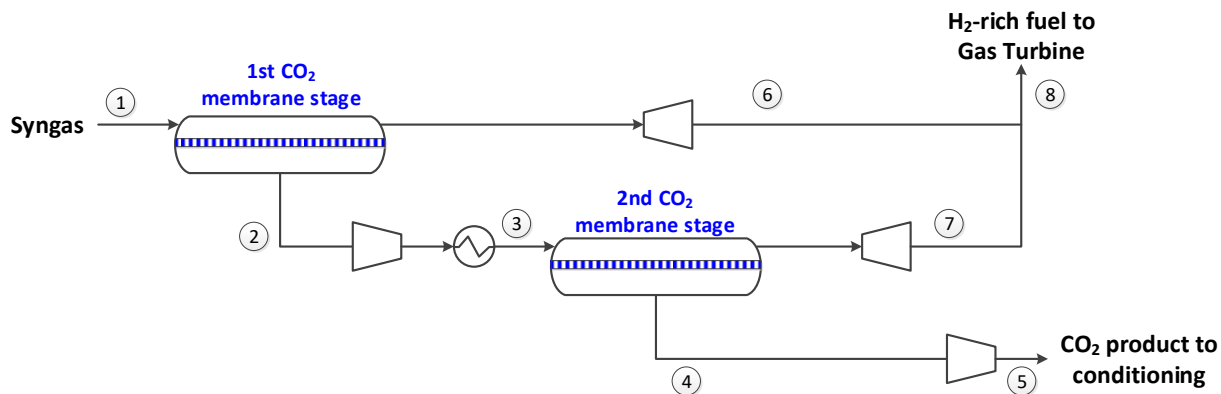| | Power requirement /MW | Membrane area /m² |
|---|---|---|
| 1st membrane stage | -1.95 | 8 920 |
| *Retentate expander* | *-1.95* | |
| 2nd membrane stage | 19.09 | 3 710 |
| *Feed compressor* | *19.78* | |
| *Retentate expander* | *-0.70* | |
| 3rd membrane stage | 13.58 | 1 939 |
| *Feed compressor* | *13.30* | |
| *Retentate expander* | *-0.28* | |
| CO₂ conditioning | 14.84 | |
| Total | 45.56 | 14 569 |

**Figure 16: Process flow diagram of the CO₂ capture process based on the CO₂-selective membrane B including stream tags**

**Table 16: Stream characteristics along the CO₂ capture process based on the CO₂-selective membrane B**

| Stream no. | 1 | 2 | 3 | 4 | 5 | 6 | 7 | 8 |
|---|---|---|---|---|---|---|---|---|
| Molar Flow /$10^3$ kmol.h$^{-1}$ | 12.03 | 5.32 | 5.32 | 4.05 | 4.05 | 6.37 | 1.26 | 7.63 |
| Mass Flow /kg.s$^{-1}$ | 68.00 | 54.93 | 54.93 | 49.73 | 49.73 | 13.07 | 5.20 | 18.27 |
| Temperature /°C | 30.0 | 30 | 30 | 30 | 30 | -15.8 | -14.1 | -15.6 |
| Pressure /bar | 28.0 | 3.8 | 28.1 | 2.3 | 150 | 14 | 14 | 14 |
| Molar composition /%mol | | | | | | | | |
| $H_2$ | 53.41 | 17.34 | 17.34 | 1.15 | 1.15 | 82.78 | 67.17 | 80.20 |
| $CO_2$ | 38.64 | 80.08 | 80.08 | 98.68 | 98.68 | 4.90 | 22.84 | 7.86 |
| $N_2$ | 5.89 | 1.91 | 1.91 | 0.13 | 0.13 | 9.13 | 7.41 | 8.84 |
| CO | 1.08 | 0.35 | 0.35 | 0.02 | 0.02 | 1.67 | 1.36 | 1.62 |
| Ar | 0.80 | 0.26 | 0.26 | 0.02 | 0.02 | 1.24 | 1.01 | 1.20 |
| Other* | 0.18 | 0.06 | 0.06 | 0.00 | 0.00 | 0.28 | 0.23 | 0.27 |

\* $H_2O$, HCL, COS, $CH_4$, etc.

**Table 17: Electrical power balance and membrane area of the CO₂ capture process based on the CO₂-selective membrane B**

| | Power requirement /MW | Membrane area /m² |
|---|---|---|
| 1st membrane stage | -2.47 | 9 373 |
| *Retentate expander* | *-2.47* | |
| 2nd membrane stage | 10.50 | 903 |
| *Feed compressor* | *10.98* | |
| *Retentate expander* | *-0.49* | |
| CO₂ conditioning | 14.83 | |
| Total | 22.86 | 10 276 |